Received 27 June 2020; accepted 19 July 2020. Date of publication 24 July 2020; date of current version 7 August 2020.

Digital Object Identifier 10.1109/OJCOMS.2020.3011171

On the Design of Multi-Hop Tag-to-Tag Routing Protocol for Large-Scale Networks of Passive Tags

CHANG LIU [1] AND ZYGMUNT J. HAAS [2,3] (Fellow, IEEE), AND ZIJING TIAN [3]

[1]Department of Mathematical Sciences, Eastern New Mexico University, Portales, NM 88130, USA

[2]School of Electrical and Computer Engineering, Cornell University, Ithaca, NY 14853, USA

[3]School of Engineering and Computer Science, University of Texas at Dallas, Richardson, TX 75080, USA

CORRESPONDING AUTHOR: C. LIU (e-mail: chang.liu@enmu.edu)

This work was supported in part by the Army Research Laboratory under Contract W911NF-18-1-0406, and in part by the National Science Foundation under Grant CNS-1763627.

ABSTRACT Recently, tag-to-tag (T2T) backscattering technique in a passive RFID system has received broad attention due to its superiority for large-scale network applications. If used to implement a Network of Tags, use of T2T communication allows inherent communication parallelism, thus supporting orders of magnitude larger capacity than centralized RFID reader-based systems. To unleash the potential of T2T communication, turbo backscattering operation enables the implementation of a multi-hop network of tags, which supports larger network coverage of a Network of Tags. However, due to asymmetric communication links and interferences among tags' transmissions in such a T2T backscattering based network, the routing protocol design has become one of the main technical challenges, especially for large-scale networks. Furthermore, the computation time of T2T routing protocols increases exponentially with the number of tags, greatly limiting the practicability of such large-scale backscattering networks. In this paper, we present the design of a *Network of Tags* model to address these challenges, and we propose novel routing protocols for three distinct types of tags with different hardware capabilities. To address the issue of computational processing time of the routing protocol for large-scale T2T networks, we propose a new scheme with linear time complexity. We evaluate and compare the performance of the proposed protocols, as well as investigate the impact of network parameters on the performance.

INDEX TERMS Backscattering communications, Internet of Things, large-scale networks, multi-hop routing protocol, network of tags, RFID passive tag, tag-to-tag communication.

I. INTRODUCTION

NOWADAYS, RFID systems have become increasingly prevalent, and it is predicted that in the future massively deployed IoT objects will be tagged for communication and control for various applications such as e-Health, Smart Cities, Smart Spaces, and Intelligent Transportation Systems. A typical RFID system, which consists of an *RFID reader* and a number of tags, has become one of the most widely used systems to facilitate automatic object identification [1]. Each tag is uniquely differentiated through its identification code, which can be recognized by the reader. RFID tags fall mainly into three categories: active, passive, and semi-passive tags. As the names imply, passive tags are solely powered by RF radiation of a reader. A typical passive RFID link between a tag and the reader operates through an interrogation process: when a passive RFID tag receives an activation signal from the reader, the signal energizes the circuits of its RFID chip, and the tag responds to the reader by backscattering the received waveform signal from the reader. What differentiates passive tags from active tags is that passive tags have neither significant energy storage nor traditional transmitters. Thus, they have advantages such as lower cost, smaller dimensions, physical flexibility, longer lifetime, environmental safety, and no need for power sources [2].

Direct tag-to-tag (T2T) communication between passive RFID tags [3] has recently attracted broad attention. When used to implement a Network of Tags, such T2T

communication allows inherent communication parallelism, thus supporting orders of magnitude larger capacity than centralized RFID reader-based systems. However, one of the main challenges in implementing a passive T2T network is that the inter-tag distances are very limited (at the centimeter level). To address this shortcoming, we propose a *Network of Tags* (*NeTa*) model [4], [5], by which two tags in a densely deployed network can communicate by relaying their communications through a chain of other tags, aiming to significantly extend the network scope.

In the *NeTa* model, the reader acts as a central controller which is responsible for calculating the optimal end-to-end communication path and then broadcasting path assignments to the network tags. We note, however, that the actual communications are not routed through the reader, thus preventing the reader from becoming a "bottleneck". The main superiority of *NeTa*, compared with a centralized network (where a centralized reader handles the actual transmissions), is that in a large-scale T2T network (i.e., with a massive number of tags), the high traffic could be offloaded by multi-hop routed T2T communications. As demonstrated in Section IV-B, with this parallelism offered by T2T transmissions, not only the overall network throughput can be significantly enhanced, but also the delays of transmission cycles can be much reduced.

For a multi-hop network such as *NeTa*, however, the backscattering environment introduces new challenges not present in the traditional multi-hop networks. The main reason that existing routing protocols cannot be applied to T2T networks is that for most other networks (e.g., wireless sensor network), the transmit power of all the communication links are assumed to be the same, resulting in symmetrical links. For a T2T network, however, the transmit power of each communication link is the backscattering power from the transmitting tag, which is based on: (1) the transmit power of the reader, and (2) the distance between that tag and the reader. Furthermore, since the tags use harvested energy from the reader to power their electronics, which operate at an extreme-low-power regime, the tags have extremely limited processing power. Thus we designed our protocols to address those limitations.

Based on our previous work in [4] and [5], we designed three T2T routing protocols for three types of tags with different hardware capabilities: (1) standard tag design (referred to as *Scenario A*), (2) tags with power detectors that are able to measure the received signal strength (referred to as *Scenario B*) [6]–[11], and (3) tags with power detectors and attenuators that can measure the received signal strength and attenuate the backscattered signal (referred to as *Scenario C*) [12]–[14]. The extra features of the latter two types of tags, as demonstrated later, can greatly reduce inter-tag interference and enhance network throughput. For example, in *scenario B* described in our work, the transmit power of the reader is considered as a variable in the protocol design. In *scenario C* described in our work, tags can attenuate their transmit power based on the protocol design. This makes the routing protocol design unique, while allows to support large throughput in spite of the limited execution power of the tags.

Another challenge in the routing protocol design is that the time complexity of the basic versions of these three routing protocols increases exponentially with the number of tags, and therefore does not apply to applications of massively-deployed RFID systems [15], [16]. To address this issue, in this work, we propose a scheme that allows replacing the exponential time complexity of the algorithms with linear time complexity. This scheme, described in Section VIII, is based on the partition of the network into regions and executing a greedy algorithm independently in each region.

We would like to point out that our routing scheme is executed at the reader (the reader solves the optimization problem), while the tags simply respond to the reader's commands. There is no direct interaction among the tags with respect to the execution of the routing protocol, so the tags do not incur any interaction overhead among the tags caused by the proposed routing scheme. This lack of overhead on the tags is one of the biggest advantages of the proposed scheme, due to the severely limited tags' processing capabilities. This is in contrast to the reader, which operates with much larger processing capabilities.

By computer simulations, we compare the network performance (capacity and computation time) of the routing protocols, as to assess the gains stemming from the tags' extra hardware capabilities. We also demonstrate how the aforementioned performances are affected by the proposed region partition scheme. The results aim to provide insights which can assist network designers in deciding which capabilities are worth implementing, based on the network performance requirement, the scale of the deployed network, and the operational parameters of the tags and the reader.

The contributions of our work can be summarized as follows: (1) we propose *NeTa*, a novel RFID network model which allows multi-hop T2T transmissions (and therefore significantly extending network coverage); (2) we propose a basic routing protocol from tags to the reader for *NeTa*; (3) we design three distinct tag-to-tag routing protocols for tags with different hardware capabilities, to maximize network capacity, while reducing inter-tag interference; (4) we evaluated and compared the three protocols, as to determine their relative improvement given the additional tag hardware; and (4) we propose a region partition scheme for the proposed routing protocols with linear time complexity as a function of the network size, so that the protocols could be used in large-scale networks.

This paper is organized as follows. Section II presents some example applications of *NeTa* to motivate this work. Section III reviews related work. In Section IV, we introduce the *NeTa* model and provide an example to demonstrate the performance improvement of this T2T network compared with the traditional (centralized) RFID system. In Section V, we present a basic protocol for routing from tags to the reader, which is used as a building block in T2T routing

protocols. Section VI and Section VII discuss the T2T routing protocol designs for simple tags and tags with advanced capabilities, respectively. Section VIII describes the proposed region partition scheme to achieve linear time complexity in large-scale networks. Evaluations and comparisons follow in Section IX. Finally, Section X concludes the paper and proposes future research directions.

II. EXAMPLE APPLICATIONS OF NETA

One of the superiorities of the proposed *NeTa* is that it allows increasing the network coverage through multi-hop routing, thus overcoming the current limitation of inter-tag distances (on the order of a couple of centimeters) in T2T communication. This may enable countless potential applications that need extended communication ranges for object interactions, human interactions, creating "communities of interest" of geographically dispersed objects, etc. In what follows, we present a number of potential application examples.

A. PANDEMIC CONTROL

As proposed in [3], one application example of passive RFID tag-to-tag communication is that when wearing bracelets with tags, tags on two people's bracelets can directly communicate by handshaking and therefore exchange information. With extended communication range of *NeTa*, however, people can retrieve information from other people/objects within a much longer distance. This means that we will be able to keep track of people who have been in close contact of others. Then if a person is later confirmed to be carrying a certain type of virus (e.g., COVID-19 virus), the retrieved data would help identify and track potential virus carriers even at a very early stage. Because of the increased *NeTa* coverage, the contact tracking can be extended to potential infection distance, such as 6 feet, for example. Although traditional RFID systems have been used to control and monitor the spread of the SARS virus [17], a significant improvement to pandemic control systems could be achieved with T2T communication networks due to an increase in network coverage.

B. SMART HOME AND SMART CITY

Smart home and smart city are among the two important research areas of Internet of Things (IoT). RFID tags, many of which are able to store and compute data or interface to sensors [18], are widely used in IoT applications when attached to various types of objects [19]–[21]. The object interaction via T2T communication then allows for proximity detection, localization, and tracking of such objects for smart home applications. This can be useful in many situations, such as locating critical everyday objects (e.g., keys or glasses), or reconfiguration of spaces based on the current locations of people who live in a house.

For smart city applications, RFID tags (with attached sensors) allow monitoring for air pollution, traffic, availability of parking spaces [22], etc. The *NeTa* can also be used in structural monitoring of buildings and bridges. Rather than using actual sensing devices, unusual conditions (e.g., cracks) can be identified simply by observing the changes in the backscattered signals.

C. TELEMEDICINE HEALTHCARE

NeTa will also find a number of applications in telemedicine healthcare system. A patient's physical activities can be monitored remotely using low cost tags [23]–[25]. The statistics of monitored data can then be used to determine the patient's health condition. With implantable arrays of tags, it is possible to extract inter-beat interval in cardiac pulses or to monitor neural activities of patients. Further, interaction monitoring can be used for sensitive objects such as blood samples or dangerous chemicals. There are also attempts to use tags for brain-machine interface. Tags can also be used to track the movement of patients in nursing homes, alerting them to potential obstacles as to prevent falls and injury.

D. PRECISION FARMING

Precision farming may benefit from *NeTa* too. For example, when animals are tagged, their activities can be monitored [26]–[28]. This can ensure adequate feeding and prevent diseases from spreading. Tags can also be used for the management of harvested crops. With *NeTa* one can retrieve information including the harvest date of crops in a bale, the field they were harvested from, the temperature, the weight, and the moisture level of each bale. *NeTa* can be used in greenhouse management as well.

III. RELATED WORK ON PROTOCOLS FOR PASSIVE RFID T2T NETWORKS

To the best of our knowledge, there is no existing literature on routing protocol design for large-scale RFID networks (as opposed to individual links), likely because T2T backscatter communication in RFID system is a relatively new and emerging area. There are related works on routing protocols for small scale passive RFID T2T networks, but even those works are quite limited and inadequate. In [29], the authors suggested that the range of T2T backscatter communication could be improved by multi-hop cooperative routing strategy. However, no detailed investigation was not included in their research. Our study in this paper provides a comprehensive investigation and proposes complete and precise protocol designs for T2T backscatter routing. In [30], a passive channel measurement technique is proposed to show the capacity improvement in T2T backscatter communication networks as compared with traditional RFID networks. In [31], an anti-collision passive channel measurement technique is proposed, where the authors focused on the channel measurement between passive tags. In [32], the authors studied the problem of jointly minimizing transmit power of readers and selecting the shortest communication route among a set of RFID readers (one reader as the source and another reader as the destination),

through multi-hop T2T communication. That work however focuses on the routing among readers utilizing T2T communication and therefore does not address how to coordinate multiple concurrent T2T transmissions, which is one of the main contributions of our work. In [33] the authors developed a backscattering T2T network using innovative tag architecture and a novel multiphase backscatter modulation technique. The routing protocol for this proposed network, however, was beyond the scope of that paper. In [34], the authors developed a distributed "optimal link cost" multipath routing protocol in the network layer and designed a MAC protocol for T2T backscatter communication. However, that work did not account for the fact that a tag's backscattered power is strongly affected by the distance between the tag and the reader. Indeed, transmission range is the major difference between T2T backscatter communication and communication in sensor networks. Our work provides a detailed analysis for communication range constraints in passive RFID T2T networks and shows the optimized routing protocol designs considering this constraint.

IV. SYSTEM MODEL

We consider a passive RFID T2T *NeTa* model consisting of a reader and passive RFID tags, which allows the implementation of a multi-hop-routed network. The reader is placed among tags which are uniformly distributed throughout the network coverage area. In this section, we first introduce the proposed *NeTa* model, and then demonstrate its improvement in network performances compared with conventional RFID systems.

A. THE NETA MODEL

One of the key challenges in the design of current RFID T2T networks is the limited inter-tag distance. The main culprit is the fact that in a T2T network, each tag undergoes a new backscattering operation, in addition to the tag's backscattering losses. This challenge is, in particular, problematic for large-scale dense networks, where a transmission from the source tag to the destination tag is likely to undergo a large number of hops. Note that according to FCC regulations (Part 15, Section 15.247 [35]–[41]), the maximum transmit power of an RFID reader is 1 Watt, and thus cannot be arbitrarily increased to improve the transmission distances. To address this issue, we rely on our proposed *turbo backscattering operation* (TBO) [4]. For completeness, we demonstrate here that, using the TBO, inter-tag distances can be significantly enhanced. To increase the coverage of a network of tags, the TBO should be used together with multi-hop routing. The fundamental principle of TBO is as follows: the reader transmits an RF waveform (referred to as *Continuous Wave* (CW)) containing power and possibly commands to individual tags instructing each tag when it is scheduled to backscatter to the next-hop receiving tag. Upon receiving this CW, a tag decodes the commands it receives and then backscatters signals containing transmitted data to its neighbors. The neighbor tags will decode the backscattered signal

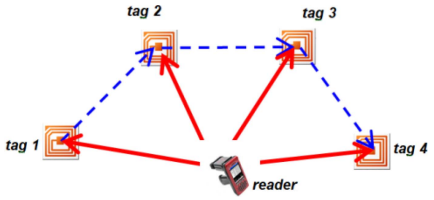

FIGURE 1. A simple example of *NeTa*. Solid arrows represent CW and dashed arrows represent flow of information.

by the first tag and, using a new CW from the reader, forward the signal to the next hop. Such an operation is similar, in concept, to the "decode and forward" operation [42], to be distinguished from "amplify and forward" [43]. However, the main distinction of *NeTa* from the "decode and forward" schemes is in the fact that, in *NeTa*, the tag's reply signal is modulated on a power waveform received from the reader (i.e., it is backscattered using a new CW on each hop), rather than using the transmitter's own carrier signal generated with the node's own power source. Accordingly, in our discussions in this paper, we consider standard passive tag operations, i.e., the tags do not have a traditional transmitter or energy storage. However, such tags are used in our work in a different manner; i.e., a backscattered wave by a tag can be received and decoded by another tag, as if the backscattered wave were received directly from a reader. To guarantee the feasibility of T2T data transmission, passive tags should have a memory to store the data received and a decoder that can decode the received packets. The chips inside should be able to determine if the messages received need to be dropped or transmitted, according to the commands broadcasted from the reader. An example of the hardware design of the passive tags is provided in [44], which contains a controller, a cyclic redundancy checker, a transmitting buffer, a pseudorandom number generator, a slot counter and a memory.

To better demonstrate how *NeTa* model works, we consider an example shown in Fig. 1 where *tag 1* needs to communicate information to *tag 4*. Upon receiving a transmission from *tag 1*, *tag 2* decodes it, and then backscatters a "fresh" CW power signal from the reader, after the signal is modulated with the decoded information. Upon receipt of the backscattered signal by *tag 3*, the same operation is then repeated for transmission from *tag 3* to *tag 4*.

One of the main concerns with the implementation of *NeTa*, such as that shown in Fig. 1, is the effect of interference from CW on the reception of backscattering signals by tags. For instance, in the example in Fig. 1, while *tag 2* receives the backscattered signal from *tag 1*, it also receives the reader's CW, which may cause interference to the reception at *tag 2* of the backscattered signal from *tag 1*. This interference is of particular concern because the backscattered signal (e.g., by *tag 1*) is significantly weaker than the CW signal, due to the signal's backscattering losses at *tag 1*. To address the effect of the CW interference, *tag 2* has to have a way to separate the CW signal from the backscattered signal from *tag 1*, which could be done in a number of ways [45], [46].

For simplification of our derivations, we assume a number of assumptions, all of which are commonly used in other works in this area (we include representative citations): (1) tags are not mounted on any surface, (2) all antennas (of tags [47]–[52] and readers [53]–[60] are isotropic radiators with 0 *dBi*, and (3) the T2T network is deployed in an open space, so that multi-path and shadowing phenomena could be neglected, and the propagation attenuation exponent $\gamma = 2$. Based on a modified Friis equation [61], for tags outside the near-field zone of the reader, the received power P_p of a CW at a tag transmitted by the reader can be calculated as:

$$P_p = P_t \cdot \left(\frac{\lambda}{4\pi r_r}\right)^2, \tag{1}$$

where P_t denotes the transmit power of the reader, λ denotes the RF wavelength, and r_r denotes the reader-to-tag distance. This received CW is next modulated by the tag with the tag's information and backscattered, allowing reception at the next tag. The received power at the next tag, P_r, can be expressed as:

$$P_r = P_p K \left(\frac{\lambda}{4\pi r_t}\right)^2 = P_t K \left(\frac{\lambda}{4\pi r_t}\right)^2 \left(\frac{\lambda}{4\pi r_r}\right)^2, \tag{2}$$

where r_t denotes the inter-tag distance, and K denotes the backscattering coefficient, i.e., the factor that represents backscattering power losses, inclusive of the effect of impedance mismatch on the re-radiated power [62]. We assume that all the passive tags in the T2T network have the same sensitivity $P^{tag}_{r,min}$. Rewriting eq. (2) with the condition that $P_r = P^{tag}_{r,min}$, yields:

$$r_t \cdot r_r = \left(\frac{\lambda}{4\pi}\right)^2 \cdot \sqrt{\frac{KP_t}{P^{tag}_{r,min}}}. \tag{3}$$

For equations (1), (2), and (3) to be valid, we need to guarantee that the distance r_r and r_t are in the far field region, [63] where both the inter-tag and reader-tag distance should be larger than:

$$d = \frac{2D^2}{\lambda}. \tag{4}$$

For reader-to-tag distance r_r, since the antenna size of a reader is typically 0.3 m [64], we obtain from eq. (4) that $r_r > 0.18\ m$. For the inter-tag distance r_t with the antenna size of a tag of 10 cm, we obtain that $r_t > 0.02$ m.

As an example, consider the case in which $K = -10$ dB, the RF frequency $f = 300$ MHz (UHF frequency as used in [65]), $P_t = 1$W, and $P^{tag}_{r,min} = -20$ dBm. A continuous multi-hop T2T path (i.e., a path consisting of a sequence of T2T links) can be established as long as the tags are sufficiently densely distributed. The range that a reader can power a tag is typically much further than inter-tag distances (i.e., $r_t \ll r_r$). If we choose $r_r = 1.25\ m \gg 0.18\ m$, the inter-tag communication should be no larger than 0.499 m according to eq. (3). On the other hand, since the far field distance for inter-tag is 0.02 m, we can deploy adjacent tags with a distance between 0.02 m and 0.499 m. Note that the inter-tag distances can be further improved by advanced hardware (e.g., by reducing $P^{tag}_{r,min}$).

Next, we investigate the limitation of the network size that a reader can communicate with (including reading from and writing to) all the tags. We first note that the sensitivity of a RFID reader is typically significantly higher than that of an RFID tag, i.e., $P^{reader}_{r,min} \ll P^{tag}_{r,min}$.[1] In order to determine the network size limitation, we assume that the tag furthest away from the reader is at the maximum distance of r_r. Substituting $P_p = P^{tag}_{r,min}$ into eq. (1), we derive that the downlink (i.e., from the reader to a tag) range $r^{downlink}_r = \frac{\lambda}{4\pi} \cdot \sqrt[2]{\frac{P_t}{P^{tag}_{r,min}}}$. To obtain the direct uplink (from a tag to the reader without multi-hop relaying) range, we substitute $P_r = P^{reader}_{r,min}$ and $r_t = r_r = r^{uplink}_r$ into eq. (2), and obtain that $r^{uplink}_r = \frac{\lambda}{4\pi} \cdot \sqrt[4]{K \cdot \frac{P_t}{P^{reader}_{r,min}}}$. Using the derivations above and assuming that the sensitivity of a reader $P^{reader}_{r,min} = -75$ dBm [66]–[71], we can calculate that $r^{downlink}_r \cong 25$ m and $r^{uplink}_r \cong 18.7$ m for the example above. We emphasize that whether a system is an uplink− or downlink−limited is strongly affected by the system parameters, such as the sensitivities of the tags and the reader, which are functions of the continually-advancing technology. In our scenario, to allow a larger coverage area, the network could utilize direct downlink transmission,[2] while the uplink transmissions are multi-hopped back to the reader. Thus, in such a network architecture, the reader has a global view and control over a large coverage area of the tags, and therefore can be utilized to determine the optimal routes as well as to schedule the tags' transmissions, while the actual transmissions are multi-hopped among the tags, bypassing the centralized reader.

B. MOTIVATION FOR THE NETA MODEL

One could ask what the need for multi-hop communication is, if a single reader can talk directly to a substantial portion of the network tags. Indeed, it may be possible to design a T2T network, where the reader would act as a centrally placed "router" that facilitates exchanges of information among the tags. However, with a large number (e.g., in the hundreds or thousands) of tags, such a reader acting as a centralized router would become a major "bottleneck" to the communications among tags. With the introduction of *NeTa*, the traffic that the reader would need to handle could be offloaded by multi-hop routed communications among the tags. Therefore, the overall network throughput can be significantly enhanced due to the *parallelism* offered by the

1. This is due to the fact that a passive tag requires energy power the electronics and due to the fact that a reader is typically equipped with more sophisticated and expensive electronics.

2. In this paper, when referring to tags, we use interchangeably the terms "backscatter" and "transmit", since the tags are passive, thus tags' transmissions are generated by backscattering energy of the reader's CW.

inter-tag communications.[3] Compared with the conventional RFID network in which all the information is transmitted through a centralized reader, our *NeTa* model for inter-tag communication has an impressive improvement in network performance in terms of throughput and delay. Indeed, our *NeTa* model, which allows multi-hop T2T transmissions, can improve the number of concurrent transmissions on the order of hundreds to thousands times. Section IX demonstrates the experimental capacity analysis. Another superiority of the *NeTa* model is that it reduces delays of transmission cycles, as shown by the following example.

Let's assume that in our system there are n tags in total and each tag requests to transmit a message to another tag. In the *centralized RFID system*, the reader starts to poll the tags for transmission requests. We assume that each poll requires L_1 bits of information to be transmitted. A poll is used by the reader to send the ID of the polled tag, by the tag to respond with the ID of its destination possibly with additional information such as the amount of data that the tag wishes to transmit. After the poll phase is completed, the reader sends a transmit schedule to the tags, which requires time τ. The reader then enters the forwarding phase, which starts by receiving a message from the first source tag, which contains L_2 bits, and forwarding the message (again, L_2 bits) to the target first tag. This forwarding phase repeats n times, once for every source tag in the system. Thus, the total time of transmissions for this centralized RFID system is:

$$T_1 = \left(\frac{L_1}{C} + \frac{L_2}{C} + \frac{L_2}{C} + \tau\right) \times n, \tag{5}$$

where C denotes the data rate of the network transmissions.

In our *NeTa* model, firstly, all the transmission path assignments are calculated before the transmissions commence. The polling phase needed to convey all the requests to the reader from the n tags requires the same time of $\frac{nL_1}{C}$. We assume that it takes ω seconds to execute the paths' finding algorithm. The reader then broadcasts the paths assignment messages to all the tags. We assume that the length of paths' assignment message for each tag is L_3 bits, and the time for all the tags to receive the paths' assignment message is, therefore, $\frac{nL_3}{C}$. The time needed for data transmission process depends on two parameters: (1) the maximum number of hops J for each transmission to reach its destination, and (2) the average number of slots k that each tag needs to wait for other transmissions in progress; i.e., $k = \frac{n}{m}$, where m denotes the number of concurrent communications in the system. The time of the data transmission phase is then $\frac{kJL_2}{C} = \frac{nJL_2}{mC}$. Thus, the total time for serving the n tags in the *NeTa* network is:

$$T_2 = \frac{nL_1}{C} + \omega + \tau + \frac{nL_3}{C} + \frac{nJL_2}{mC}. \tag{6}$$

As an example, we set the parameters as follows: radius of the area is 5 m, $L_1 = 5$ kbits, $C = 1$ Mb/s, $L_2 = 20$ kbits, $\tau = 100\mu$s, $L_3 = 2$ kbits, and $J = 4$. For the value of k and ω, we rely on our results in Section IX (Figs. 8 and 9). We then calculate T_1 and T_2 to demonstrate the improvement in the transmission time delay. Fig. 2 shows the estimated total transmission time for the "*Centralized RFID*" system and our *NeTa* network as a function of the numbers of tags in the network. From the figure, we observe the impressive reduction in the total delay of the distributed *NeTa* approach.

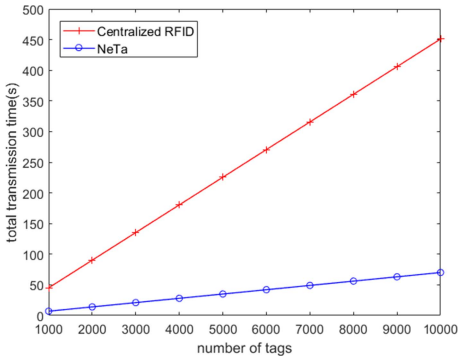

FIGURE 2. Delay comparison between NeTa and a Centralized RFID network.

It is also worth noting that high-performance readers are typically expensive devices (e.g., the cost of an RFID reader at the time of this paper is in the thousands of dollars), thus their use should be minimized. Use of multi-hop routing on the uplink in *NeTa* would allow using fewer and possibly cheaper readers. Furthermore, the function of CW power source could be provided by much simpler and cheaper devices, which could be spread throughout the coverage area, thus replacing some of the readers, while a more expensive reader could be used only as an ingress and egress element to connect the *NeTa* to the rest of the world.

In the rest of the paper, we consider the architecture where the reader serves as a central controller (rather than as a router) to determine routes and schedule tags' transmission times within our *NeTa* model. Our proposed routing protocol consists of two steps. First, the reader identifies all the tags within its coverage area and determines the uplink routing paths for each tag, so that the poll signals between tags and reader are supported. This protocol is presented in Section V. Thereafter, the reader discovers the neighboring tag information and determines direct T2T transmission schedules, as described in Sections VI and VII. Then in Section VIII, we introduce a novel region partition scheme to support low time-complexity for large-scale RFID systems.

V. THE BASIC ROUTING PROTOCOL FROM TAGS TO READER

This section presents a basic routing protocol from tags to the reader, with the purpose to: (1) discover all the tags that are directly reachable by the reader on the downlink and either directly or indirectly reachable through a certain number of hops on the uplink, and (2) determine a routing path on the uplink for each discovered tag.

3. Furthermore, with NeTa, the network coverage can be increased when the uplink is the limiting distance

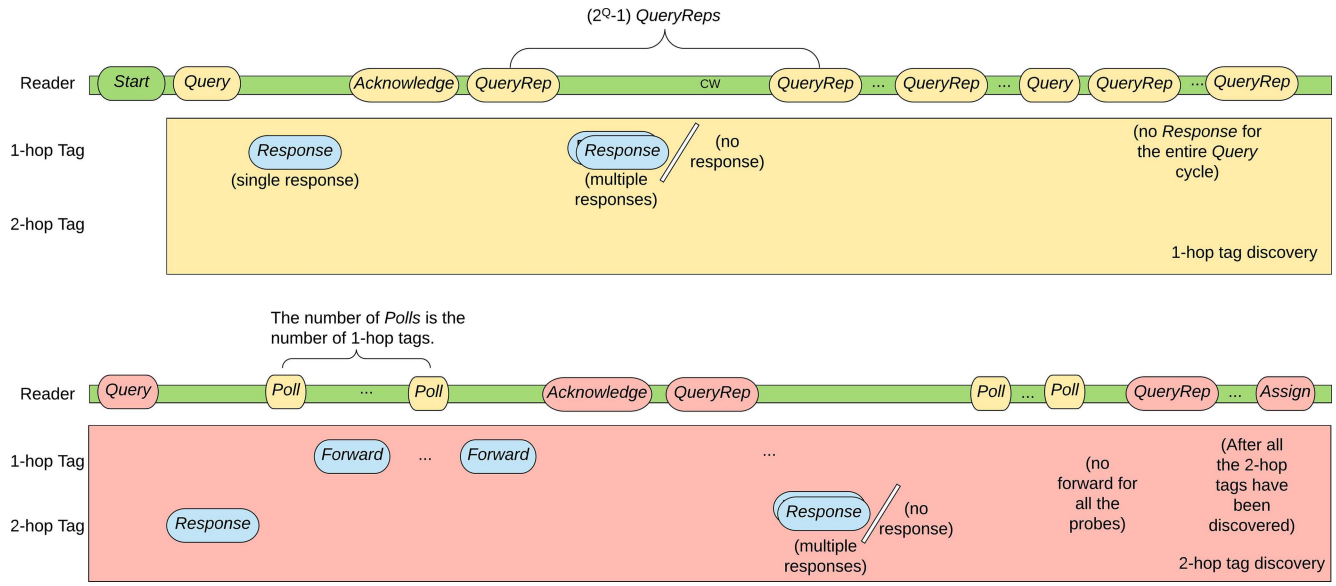

FIGURE 3. A time-line diagram for the discovery process of 1-hop and 2-hop tags. Green commands/CW indicate that the reader fully operates at its maximum power. Yellow commands indicate that the reader transmits at a level to reach the 1-hop tags. Peach commands indicate that the reader transmits at a level to reach the 2-hop tags.

To simplify the protocol operation, the network coverage area is divided into annulus hop layers. Each i-hop layer represents "one hop" of the uplink path routing (the tags can be directly reached by the reader on the downlink, though). In other words, the reader can directly communicate with tags in the 1-hop layer on both uplink and downlink, but in an i-hop layer for $i \geq 2$, tags need at least i hops to route back to the reader. The width of each annular layer depends on the density of the tags; i.e., the backscattering of a tag in layer i needs to be heard by at least one tag in layer $i-1$. Based on eqs. (1) and (2), we can determine the radius of each annular layer and therefore the width of each layer. From the derived results it is shown that the width of an annular layer decreases as the index of the layer increases [4], [5].

The basic routing protocol targets tags in a single hop layer at a time by setting a certain level of transmit power of the reader. We start by describing the transmit power control of the reader. Next, we present the basic discovery process. This basic protocol will be used later as a building block of *NeTa*.

A. TRANSMIT POWER CONTROL OF THE READER

Typically,[4] when the reader acts only as a source of CW and does not transmit commands, it operates at its full power to energize all the tags in the coverage area. However, when the reader broadcasts instructions to tags, we adjust the reader's transmit power so that a transmission is limited to a particular geographical region (i.e., annular layer) as described in Section IV.

In each cycle, we attempt to discover tags in a particular i-hop region. We start with the 1-hop ($i = 1$) layer and then progressively increase i to higher hop layers (in a practical network setting, the maximal i will be 4∼5). To achieve this, the transmit power of the reader when sending commands should be slightly larger than the theoretical transmit power needed to reach the outer edge of a hop layer (as determined by the Friis formula) to account for environmental factors (such as obstacles, multipath, etc.) that might cause extra attenuation. Note that with the adjusted transmit power, although tags in higher hop layers may also receive commands from the reader and attempt to respond, their responses will be discarded due to the expiry of the hop counter of such transmissions. However, with the power just moderately larger than necessary for a particular layer, the transmission will not reach too far as to cause too much extraneous traffic.

B. DISCOVERY PROCESS

We now describe the general principles of our discovery process (depicted as an example in Fig. 3), which is initiated when the reader broadcasts a *start* command. To discover tags in the 1-hop region, the reader sends a *Query* message to tags in the region, with the 1-hop tags replying with a message *Response* to identify themselves to the reader.[5] When a *Query* is sent for the first time to an i-hop region, some tags may be discovered while some other tags may collide in the selected slots. If a tag is discovered, the reader sends an *Acknowledge(tag1ID)* message to the discovered tags with

4. Power control of the CW could be used to further reduce interference on tags' transmissions, in addition to schemes such as in [45], [46], but we omit such a discussion here as being beyond the scope of this paper.

5. Since the reader coordinates all tags' transmissions, when a tag is scheduled to transmit (either to the reader or to another tag), the reader sends a CW to facilitate such a transmission. Since all such tag transmissions are facilitated by the reader, for simplicity, we often omit the statements that the reader sends the CW when a tag is to transmit.

the corresponding tagIDs, so that every tag receiving the *Acknowledge(tag1ID)* message with its matching tagID will cease from responding to future *Query* messages. The discovered tags are acknowledged and therefore remain silent for future *Query* messages. The reader then repeatedly sends out *QueryRep* messages to the same *i*-hop region until all the tags in the 1-hop region have been presumably discovered (e.g., no responses received to a subsequent *Query* message during a certain number of consecutive *QueryRep* cycles). This is so, since with a large enough frame, it is very unlikely that all the nodes collide at a same time slot so that no tag is "found" within that cycle. Note that although there exists a possibility of missed tags, the missed tags can still be discovered in following *Query* cycles since such undiscovered tags have not received an *Acknowledge* message. After the discovery in the 1-hop layer is complete, the reader proceeds to discover tags in the 2-hop region by sending *Query* messages with an increased power to reach the 2-hop region. The discovered tags in the 1-hop region remain silent, but tags in the 2-hop region reply. Any tag (identified by *tag1ID*) in the 1-hop region that hears such a reply from a 2-hop tag, records such a reply message, and forwards the reply message as well as its own information directly to the reader (such a message is named *Forward*) when probed next by the reader's *Poll(tag1ID)* message. When a tag's response is successfully forwarded to the reader, the reader sends an *Acknowledge(tag2ID)* message to every newly discovered 2-hop tag (with *tag2ID)*. After receiving all messages from the 2-hop tags, the reader then determines which 1-hop tag will be responsible for relaying each 2-hop tag's transmissions, by sending an *Assign(tag1ID, tag2ID)* message to each 1-hop tag (with *tag1ID*) to inform it which 2-hop tag (with *tag2ID)* it is responsible relaying for. Similarly, the process continues to discover and determine routing for tags in the next *i*-hop region, utilizing the previously determined routing of the lower hop regions. We note that in this protocol the reader takes care of most of the operations, while the tags' operations remain relatively simple.

An example of the discovery process of tags in both 1-hop layer and 2-hop layer is demonstrated as a time-line diagram in Fig. 3. Both situations of successful transmissions (i.e., only one tag responds) and unsuccessful transmissions (i.e., collision or no response) are shown.

VI. T2T ROUTING PROTOCOL FOR SIMPLE TAGS

For the T2T routing protocol design, we consider tags with several different hardware capabilities: (1) tags that are not able to either measure their received power nor attenuate their backscattered power (i.e., the traditional tag design), referred to as *Scenario A*; (2) tags capable of measuring their received power, but not capable of attenuating their backscattered power, referred to as *Scenario B*; and (3) tags capable of both measuring their received power and attenuating their backscattered power, referred to as *Scenario C*. We refer to the tags of the first type and those of the last two types as *simple tags* and as *advanced tags*, respectively. In this section, we propose a centrally-executed protocol for distributed routing among the simple tags. The routing protocol design for the advanced tags is presented in Section VII.

The main challenge of T2T routing design is the interference of one tag transmission on another. In other words, although the existence of a link between two nodes can be easily determined in the absence of other transmissions, the existence of the link when other transmissions are present is more difficult to determine. Specifically, a transmission can cause interference even if the transmission by itself does not create a viable link to the target tag. Furthermore, even if any single interfering transmission cannot create sufficient amounts of interference for a particular link, the sum of a number of such interfering transmissions may suffice to disable reception at the receiver of that link. In the proposed protocol, we aim to coordinate transmissions of tags to reduce the effect of interference and to enhance the network throughput (i.e., the total number of concurrent transmissions). Next, we describe the steps of the proposed T2T routing scheme.

A. NEIGHBOR DISCOVERY

The routing protocol starts with the Neighbor Discovery phase to establish a "neighbor table"; for each particular tag, the table contains the IDs of both: the tag's one-hop receivable neighbors (i.e., tags located close enough, so that their backscattering could be received and decoded) and its interfering neighbors (i.e., tags which, when they transmit, can cause significant interference at the particular tag).[6] The interfering neighboring tags should be disabled from transmitting when the particular tag receives. To achieve this, during the Neighbor Discovery process, the reader transmits CW at two different power levels: P_H and P_L, where $P_L < P_H$. To be more specific, the reader transmits CW at a relatively lower power level P_L to detect possible communication links among the tags, while the reader transmits CW with the higher power level P_H to discover potential interfering links. The rationale behind this approach is as follows. When the reader transmits CW at the lower power level P_L (which is also the level that will be used for energizing links for communication), it can discover valid links. When the reader transmits CW at the higher power level P_H, it discovers the tags whose transmission power (which may be insufficient to establish a link when the reader transmits at the lower power level P_L) can still cause sufficient interference at the receiving tag when it transmits at the same time as some other tags. In other words, the difference $P_H - P_L$ provides a margin to protect against the additive nature of interference from multiple tags. We refer to the links discovered by P_L and P_H as *transmission links* and *interfering links*, respectively.

6. We emphasize again that, due to the particular backscattering environment, in general, the neighbor tables are is not symmetrical; e.g., if a link from tag *i* to tag *j* exists, this does not ensure that a link from tag *j*to tag *i* exists too.

Upon receiving all the needed information, the reader combines the information to construct: (1) a connection map (a map with all the possible connection links among the tags) which will be used to find routing paths, and (2) a collision map (a map with all possible interferences) to inhibit interfering transmissions and protect the ongoing transmissions. The connection map and the collision map are then used to compute messages' routings and the corresponding tags' transmission schedule by the reader, depending on which tags have messages to transmit and the messages' destinations, so as to maximize the network throughput.

B. THE PROPOSED T2T ROUTING PROTOCOL

The scheduling of T2T transmissions part of the routing protocol is arranged in cycles, and each cycle consists of two parts: *Message Discovery (MD)* and *Message Routing (MR)*. During the *MD*, the reader queries individual tags for newly generated messages during the previous cycle. When a message is generated at a tag, the identity of the message is transmitted to the reader by the tag. At the beginning of each *MR*, the reader chooses the subset of tags to transmit in this *MR*, instructing those nodes to transmit thus avoiding collisions among the transmitting tags and mitigating tag interference. After the selected nodes transmitted, the reader adjusts the list of pending messages per each tag. Note that in each *MR* a tag can only transmit up to one message, although it may have multiple messages queued for transmission.

The main part of the proposed T2T routing protocol is the choice of the tags to transmit in an *MR*, which is determined as follows. We assign weights to the pending messages, based on their priorities, the path lengths to their destinations, and the messages' already encountered delays. In general, a message with a larger weight is more likely to be chosen for transmission sooner (i.e., in an earlier cycle). The weight of the j^{th} message at tag i is calculated as:

$$w_{i,j} = p_{i,j}\big(1 + d_{i,j}\alpha\big)\big(1 + h_{i,j}\beta\big), \tag{7}$$

where $p_{i,j}$ denotes a priority parameter indicating the importance of this message, and α and β denote the relative importance of the delay and the path length, respectively, of the message. The term $(1+d_{i,j}\alpha)$ is used to avoid "starving" messages, where $d_{i,j}$ denotes the total number of cycles that the j^{th} message has been waiting (already delayed) at tag i. In other words, for each cycle that transmission of a message is inhibited, the message's $d_{i,j}$ parameter is increased by one. The term $(1+h_{i,j}\beta)$ is used to increase the weights of messages with longer paths, as to speed up messages that need to travel "further" (in terms of the number of hops). Here $h_{i,j}$ denotes the number of hops of the shortest routing path[7] for the message.

We propose an algorithm to select a subset of messages for transmission in the current cycle's *MR*, such that the transmissions of those tags do not interfere one with another, and as to maximize the sum of the weights of the selected messages to transmit. The algorithm uses binary variables x_i and $c_{i,j}$ to signify the transmission state of a tag i and that of the j^{th} message at tag i, respectively. When $x_i = 1$ the tag is chosen to transmit, and when $x_i = 0$ the tag holds its messages. Similarly, when $c_{i,j} = 1$ the j^{th} message is transmitted at tag i, and when $c_{i,j} = 0$ the j^{th} message is withheld.[8] The problem is then formulated as a binary optimization problem:

$$\begin{aligned}
&\text{Maximize: } F(\mathbf{x},\mathbf{c}) = \sum x_i c_{i,j} w_{i,j},\\
&\text{Subject to: C1: } \forall_i : x_i \in \{0,1\}, \forall_{i,j} : c_{i,j} \in \{0,1\},\\
&\qquad \text{C2: } \forall_i : x_i \sum_j \left(c_{i,j} \prod_{k\neq j} \overline{c}_{i,k} \right)\\
&\qquad + \overline{x}_i \prod_j \overline{c}_{i,j} = 1,\ j,k \in \Phi_i,\\
&\qquad \text{C3: } \forall_{i,j} : g\Big(c_{i,j}, \sum x_m\Big) = 1, m \in q_{i,j},
\end{aligned} \tag{8}$$

where $\mathbf{x} = [x_1, x_2, \ldots, x_n]$, $\mathbf{c} = [c_{i,j}]$, and $q_{i,j}$ is the set of the interfering tags for the destination tag of the message $c_{i,j}$. The function $g(x,y) = x\overline{y} + \overline{x}$ expresses the constraint that y cannot occur when x occurs. Φ_i denotes the set of the indices of messages queued at tag i. The constraint C1 indicates that x_i and $c_{i,j}$ are binary. The constraint C2 ensures that each tag can transmit at most one message in each *MR*, and that a tag transmits if and only if at least one of its messages is selected for transmission. Constraint C3 represents the collision protection constraints for all the messages; i.e., for each message being transmitted, the next-hop receiver should be protected from potentially interfering transmissions. The *interfering tags* refer to tags (i.e., $q_{i,j}$) that can interfere with the next-hop receiving tag when the message $c_{i,j}$ is transmitted.

The above problem can be solved by a greedy algorithm. First, all the messages are sorted by their weights $w_{i,j}$ in a descending order. We first choose the message with the largest weight (and therefore the corresponding source tag) to transmit and add it to the transmitted message list T, which includes all the messages that have been chosen to transmit. Then we check the next message on the weight-sorted list and determine whether the corresponding message could be transmitted. If that message does not violate any constraints (C1 − C3) with the transmissions already in set T, it is added to set T, or otherwise it is rejected. Similarly, the algorithm then proceeds sequentially to the next message with the next largest weight. Note that being a heuristic, the greedy algorithm may not always be optimal. However, it is exceptionally time efficient compared with other traditional methods (e.g., genetic algorithm or branch and bound method).

7. As there can be multiple paths for each message, the shortest path is used to calculate the value of $h_{i,j}$.

8. The reason for differentiating among the different messages at tag i waiting for transmission is that the individual messages may differ in the values of their parameters in (7).

Note that, in general, there might exist multiple routing paths between a pair of tags, although the reader will determine a "preferred" path based, for example, on the paths' lengths (i.e., number of hops) and possibly other parameters. The optimization problem described above is formulated for messages on their preferred routing paths, as determined by the reader. Therefore, the algorithm could be further improved by allowing nodes, which "overhear" a transmitted message, to retain a copy of such a message, and to try to route such a copy on a non-preferred path. The basic principle is as follows: after the optimization of (8) is completed, the reader sequentially checks each of the other copies of the messages to see if they could still be transmitted, without affecting the transmissions of the selected messages. This can be done in the following three steps: (a) encoding the constraints of transmitting a copy (e.g., two messages could not be transmitted by a same tag in the same *MR* cycle), (b) substituting the selected values of variables (tags and messages) that were already chosen to transmit or not to transmit, and (c) seeing whether transmitting a copy violates any of the constraints C3 in (8). The order of the messages to be checked is as follows: (a) copies of all the messages not selected for transmission, starting from the shortest path to the longest paths, until all the copies are checked, and (b) the copies of messages which are already being selected for transmission, starting from the shortest path to the longest paths until all the copies are checked. Once a message or its copy reaches the message's destination, all the other copies of this message are erased from the nodes. By accommodating this modification, the algorithm continues to first select messages for transmission on their preferred routes, and also allows copies to be transmitted, if such transmissions do not affect the selected messages on their primary paths. We summarize the steps of Algorithm 1 below and present a simple example of the protocol in the Appendix.

Algorithm 1 Routing Protocol for Scenario A

Inputs: T: message list that includes all the messages that have been chosen to transmit.
Step 0: The reader queries individual tags for newly generated messages. $T = \{\}$.
Step 1: Assign weights to the pending messages.
Step 2: Sort all the messages in a descending order of weights.
Step 3: Add the message with the largest weight to T.
Step 4: Check the next message on the weight-sorted list. If that message does not violate the constraints C1-C3 in (8) with the transmissions in set T, add it to set T. Otherwise it is rejected. Proceeds sequentially to the next message with the next largest weight until all the messages are checked.
Step 5: The reader sequentially checks each of the other copies of all the messages not selected for transmission, and then each of the copies of messages which are already being selected for transmission (starting from the shortest path to the longest paths), if they could still be transmitted without affecting the transmissions of the selected messages.
Step 6: Once a message or its copy reaches the message's destination, all the other copies of this message are erased from the nodes.

VII. T2T ROUTING PROTOCOL FOR ADVANCED TAGS

In this section, we present T2T routing protocols for *NeTa* with advanced tags for *Scenario B* and for *Scenario C*. In Scenario B, tags are able to discover all interference patterns as part of the neighbor discovery process, allowing better (than in Scenario A) routing decisions. In Scenario C, a tag can further reduce interference by attenuating its backscattering power to the minimum power that it needs to reach its intended receiving tag, and therefore improving the network capacity.

The notations we use in Scenario B are slightly different from those in Scenario A. In Scenario B, the messages also need to be labeled with the next hop destination ID. This is because in Scenario A, the strength of the reader's CW is fixed and thus the connectivity and collision patterns are also fixed. In Scenarios B, however, the reader's CW power is selected as part of the optimization process. Therefore, such a connectivity map cannot be constructed in Scenario B, as it depends on the reader's power (i.e., there could be a different map for each level of the reader's CW power). Thus, as part of the optimization in Scenario B, the messages at each tag i need to be also indexed based on their next-hop destination, as to ensure that a message could, indeed, be delivered with the selected reader's power. Therefore, while in Scenario A, a message number j from tag i was labeled as c_{ij} (and the destination is only used in the determination of the interference conditions in C3 of (8)), in Scenario B, a message number j transmitted from tag i to its next-hop destination tag k is labeled as $c_{(i,k)j}$. This argument also applies to Scenario C, where the possibly-attenuated backscattered power of a tag (and, thus, the existence of a link to a message destination) is determined by the optimization process.

A. T2T ROUTING PROTOCOL FOR TAGS WITH ABILITY TO MEASURE THEIR RECEIVED POWER

The basic idea behind Scenario B is that the reader's CW power should be chosen properly, so as to maximize the network throughput together with the routing decisions. Said differently, on one hand, if the power of the reader is too small, there are too few transmission links possible, leading to a decrease in throughput. On the other hand, if the reader's power is too large, there are lots of potential links, but the many links also create excessive interference, effectively disabling many of these potential links. The goal is to find the optimum reader's power, so as to maximize the (weighted) throughput. We assume in this section that, in order to successfully receive a transmitted signal, a tag needs to receive the signal with *Signal-to-Interference Ratio (SIR)* of at least η (here η denotes the selected value of SIR threshold). The determination of η depends on, among other things, the modulation scheme of the tags' signaling.

Since in Scenario B the reader's transmission power is not fixed, the Neighbor Discovery process in Scenario B is also different than that of Scenario A. In Scenario B, when the reader attempts to discover transmission links and interfering links in the neighbor discovery process, the reader transmits CW at its maximum power P_t^{max}, so that all the potential links could be discovered. With the tags capable of measuring their received power, it can be determined at what power the reader needs to transmit its CW for a particular link to exist. Specifically, when the reader transmits CW at its maximum power P_t^{max}, and the backscattered power from tag i is received by tag k with power P_r, the reader can calculate that the link from tag i to tag k exists if the reader's transmit CW power is at least:

$$P_{i,k} = P_{r,min}^{tag} P_t^{max} / P_r, \tag{9}$$

where $P_{r,min}^{tag}$ is the minimum required received power by a tag for successful detection (i.e., the tag's sensitivity; for example, $P_{r,min}^{tag} = -20$ dBm [72]–[76]. Then, using eq. (9), the reader can build a power matrix for Scenario B, $\mathbf{P^B} = [P_{i,k}^B]$, where each element $P_{i,k}^B$ represents the minimum needed reader's CW power for the link from tag i to tag k to exist.

Moreover, based on the matrix $\mathbf{P^B}$, given the transmission power of the reader, the interference created by a transmission of another tag (i.e., when the transmission is not destined to the tag) can also be determined. For example, when the reader transmits CW at P_t^{max}, if the backscattered signal from tag i is received by tag k with power P_r, one can calculate that when the reader transmits CW at some power $P_t (P_t = P_t^{max})$, the received power at tag k, $P_{i,k}^r$, is $P_{i,k}^r = P_r P_t / P_t^{max}$. Practically, given $P_{i,k}^B$ (from the matrix $\mathbf{P^B}$), $P_{i,k}^r$ can be calculated by the reader as:

$$P_{i,k}^r = P_{r,min}^{tag} P_t / P_{i,k}^B, \tag{10}$$

assuming that $P_{i,k}^B \leq P_t^{max}$ (or, alternatively that $P_{i,k}^r \geq P_{r,min}^{tag}$); i.e., that the link actually exists.

As part of the Neighbor Discovery process, the reader creates the matrix $\mathbf{P^B} = [P_{i,k}^B]$, based on the measurements that the reader obtains from the tags. We note that the accuracy with which the tags measure the received power, and/or transmit the power to the reader, depends on the hardware for power measurement at the tags. In practice, such power measurement does not need to be extremely accurate; e.g., increments of 1 dBm should suffice for most practical implementations.

Therefore, based on matrix $\mathbf{P^B}$, we formulate a mixed-integer optimization problem as follows. We select a set of transmitting nodes ($\{i : x_i = 1\}$) and a subset of their messages ($\{c_{(i,k)j} = 1\}$) to be transmitted, as well as the transmit power of the reader (P_t), to maximize the weighted throughput function, as part of the proposed routing protocol. Specifically,

$$\text{Maximize: } F(P_t, \mathbf{x}, \mathbf{c}) = \sum x_i c_{(i,k)j} w_{(i,k)j},$$

$$\begin{aligned}
\textit{Subject to: } & \text{C1: } \forall_i : x_i \in \{0,1\},\ \forall_{i,k,j:}\ c_{(i,k)j} \in \{0,1\},\\
& \text{C2: } \forall_{i,k,j} : g\left(c_{(i,k)j}, \bar{I}_1\left(P_{i,k}^B\right)\right) = 1,\\
& j \in \left\{1, \ldots, n_{i,k}\right\},\\
& \text{C3: } \forall_i : x_i \sum_{k,j} \left(c_{(i,k)j} \prod_{l \neq j} \bar{c}_{(i,k)l} \prod_{m \neq k} \bar{c}_{(i,m)q_m} \right)\\
& + \bar{x}_i \prod_{k,j} \bar{c}_{(i,k)j} = 1, k, m \in \Psi_i,\\
& j, l \in \left\{1, \ldots, n_{i,k}\right\}, \text{ and}\\
& q_m \in \{1, \ldots, n_{i,m}\},\\
& \text{C4: } \forall_{i,k,j} : g\left[c_{(i,k)j}, \sum_{m \neq i} c_{(m,k)q_{m,k}} \right] = 1,\\
& q_{m,k} \in \{1, \ldots, n_{m,k}\},\\
& \text{C5: } \forall_{i,k,j} : c_{(i,k)j} = 0 \text{ if } \frac{P_{i,k}^r}{\sum_{l \neq i} \left(P_{l,k}^r \cdot x_l\right)} \leq \eta,\\
& j \in \left\{1, \ldots, n_{i,k}\right\},
\end{aligned} \tag{11}$$

where $\mathbf{x} = [x_1, x_2, \ldots, x_n]$ and $\mathbf{c} = [c_{(i,k)j}]$; $I_1(P_{i,k}^B)$ denotes an indicator function s.t. $I_1(P_{i,k}^B) = 1$ if $P_t = P_{i,k}^B$, and otherwise $I_1(P_{i,k}^B) = 0$; $c_{(i,k)j}$ denotes the j^{th} message copy from tag i to tag k; the function $g(x, y) = x\bar{y} + \bar{x}$ expresses the constraint that y cannot occur when x occurs; and $P_{i,k}^r$ is calculated using eq. (10). Similarly to Scenario A, the weight of the j^{th} message copy from tag i to tag k, $w_{(i,k)j}$, is defined as $w_{(i,k)j} = p_{(i,k)j}(1+d_{(i,k)j}\alpha)(1+h_{i,j}\beta)$, where $p_{(i,k)j}$ denotes a priority parameter of the j^{th} message from tag i to tag k, and $d_{(i,k)j}$ denotes the already accumulated delay of the j^{th} message from tag i to tag k at the current tag. Ψ_i denotes the set of next-hop destinations of message copies at tag i. $n_{i,k}$ denotes the number of messages (queued at tag i) from tag i to tag k. Constraints C1 and C3 are similar to C1 and C2, respectively, in the formulated problem (8) for Scenario A (appropriately modified due to the change in notation). Constraint C2 represents that a message can be transmitted only when the transmit power of the reader suffices, so that the corresponding communication link exists. Constraint C4 indicates that if message j from tag i to tag k is transmitted (i.e., $c_{(i,k)j} = 1$), no other node transmits to the same destination node k (i.e., $c_{(m,k)l} = 0$ for $m \neq i$). Constraint C5 represents that a message cannot be successfully received when the total interference power results in SIR $< \eta$. We note that the optimization of the reader's CW power in the above problem is carried out through $I_1(P_{i,k}^B)$ and $P_{i,k}^r$ (eq. (10)).

The above formulated problem is a mixed integer nonlinear programming (MINLP) problem, which can be solved by a similar greedy algorithm as described in Section VI. In scenario B, we set P_t to be discrete values with increments of 1 dBm and $P_t \leq P_t^{max}$. This accuracy should suffice in most practical implementations, as discussed before. We then obtain solutions of $\mathbf{x}$ and $\mathbf{c}$ for each selected value of

TABLE 1. The values of $P^{B}_{i,k}$ (in dBm); row indices indicate the transmitting tags, while the column indices indicate the receiving tags. Available links are indicated by bold fonts.

	1	2	3	4	5	6	7	8	9	10
1	∞	31.7	36.7	39.2	**28.0**	31.9	42.2	38.6	**25.2**	**26.5**
2	**23.6**	∞	**26.1**	**27.1**	**25.1**	**11.8**	31.2	**28.1**	**18.2**	**23.8**
3	35.6	33.1	∞	38.2	33.2	31.3	40.3	**24.0**	33.8	32.9
4	34.6	30.5	34.6	∞	35.6	31.4	**26.8**	35.0	33.0	35.0
5	**28.7**	33.9	35.0	40.9	∞	33.0	43.5	37.6	**29.9**	**17.1**
6	**24.8**	**12.8**	**25.2**	**28.9**	**25.1**	∞	32.6	**27.8**	**19.6**	**23.7**
7	42.9	40.0	42.1	32.1	43.5	40.4	∞	42.0	41.7	43.1
8	38.6	36.1	**25.0**	39.6	36.8	34.8	41.2	∞	37.1	36.6
9	**22.3**	**23.4**	32.1	34.8	**26.4**	**23.8**	38.1	34.3	∞	**24.2**
10	**26.5**	31.81	33.9	39.6	**16.3**	30.7	42.2	36.5	**26.9**	∞

P_t. Then the optimal solution of P_t is selected to be the one which maximizes the objective function (11), with the corresponding optimal values of $\mathbf{x}$ and $\mathbf{c}$. Similar to Scenario A, the algorithm in (11) can be further improved if we allow nodes that overhear a transmitted message to retain the message's copy and try to route it on a non-preferred path. Such a further optimization assumes that the selected CW power does not further change. We summarize the steps of the protocol in Algorithm 2.

As an example, we consider a network of tags randomly distributed in a circular area with radius of 1.25 m with density of 2 $/m^2$, as shown in Fig. 4. We assume that $K = -10$ dB, the RF frequency f= 300 MHz, P_t^{max}= 30 dBm, and $P^{tag}_{r,min} = -20$ dBm. By measuring the received power at the tags as part of the Neighbor Discovery process, the reader can obtain the minimum values of the reader's transmit power $P^{B}_{i,k}$ for the link from tag i to tag k to exist (i.e., the matrix $\mathbf{P^B}$), as shown in Table 1. Note that the links with values greater than 30 dBm in Table 1 cannot exist, since the required transmit power of the reader would exceed the maximum allowable transmit reader's power P_t^{max}= 30 dBm. Also, as noted above, in practical implementations, the table will depend on the power measurement accuracy of the tags.

We assume that there are five messages that need to be sent on their preferred routing paths: $c_{(2,9)1}$ from tag 2 to tag 9, $c_{(3,8)1}$ from tag 3 to tag 8, $c_{(4,7)1}$ from tag 4 to tag 7, $c_{(5,10)1}$ from tag 5 to tag 10, and $c_{(10,1)1}$ from tag 10 to tag 1.

There are also three messages that can be sent on non-preferred routing paths: $c_{(6,5)1}$ from tag 6 to tag 5, $c_{(8,3)1}$ from tag 8 to tag 3, and $c_{(9,6)1}$ from tag 9 to tag 6. For simplicity of the description of this example, we assume equal weights for each message. By solving the MINLP problem presented above (the optimal power of P_t is searched from 20 dBm to 30 dBm with an increment of 1 dBm) and then sequentially checking if transmissions on non-preferred paths can still be sent, we obtain the optimal values of: $c_{(2,9)1}{}^* = 0$, $c_{(3,8)1}{}^* = 1$, $c_{(4,7)1}{}^* = 1$, $c_{(5,10)1}{}^* = 1$, $c_{(10,1)1}{}^* = 1$, $c_{(6,5)1}{}^* = 0$, $c_{(8,3)1}{}^* = 1$, $c_{(9,6)1}{}^* = 0$, $\mathbf{x}^* = [0, 0, 1, 1, 1, 0, 0, 1, 0, 1]$, and $P_t^* = 27$ dBm.

Algorithm 2 Routing Protocol for Scenario B

Inputs: T: message list that includes all the messages that have been chosen to transmit.

Step 0: The reader transmits at its maximum power P_t^{max} and queries individual tags for newly generated messages. Based on the measurement of received backscattered power on each tag, the reader obtains $\mathbf{P^B}$ and $\{P^r_{i,k}\}$ by calculation. $T = \{\}$.

P_t is set to discrete values with increments of 1 dBm and $P_t \leq P_t^{max}$. For each set value of P_t, do step 1 to step 5.

Step 1: Assign weights to the pending messages.

Step 2: Sort all the messages in a descending order of weights.

Step 3: Add the message with the largest weight to T.

Step 4: Check the next message on the weight-sorted list. If that message does not violate the constraints C1-C5 in (11) with the transmissions in set T, add it to set T. Otherwise it is rejected. Proceeds sequentially to the next message with the next largest weight until all the messages are checked.

Step 5: The reader sequentially checks each of the other copies of all the messages not selected for transmission, and then each of the copies of messages which are already being selected for transmission (from the shortest path to the longest paths), to see if they could still be transmitted without affecting the transmissions of the selected messages.

Step 6: Once a message or its copy reaches the message's destination, all the other copies of this message are erased from the nodes.

Step 7: Pick the value of P_t and its corresponding messages selected to be sent that maximize the weighted throughput function.

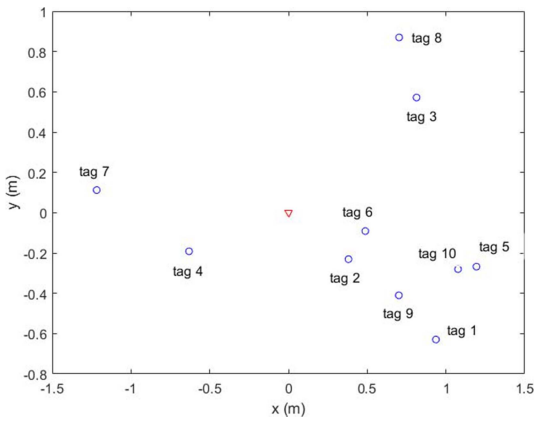

FIGURE 4. An example of a network of tags. The blue circles represent tags and the red triangle represents the reader.

B. TAGS WITH ABILITY TO MEASURE THEIR RECEIVED POWER AND TO ATTENUATE THEIR TRANSMIT POWER

In Scenario C, we consider tags to have the ability to measure their received power and to attenuate their backscattered power, so as to limit their backscattering power, and thus the interference on other links. Said differently, the backscattering power of a tag should be attenuated to result in the received power at the next-hop

tag being equal to the minimum required for reception $P_{r,min}^{tag}$ (possibly with some margin to account for unexpected interference/fading/attenuation). The main difference from Scenario B is that in Scenario C the reader always transmits at its maximum power P_t^{max} (the reader's CW power does not cause interference; see Section IV and [46]) and interference of backscattering tags is minimized through the tags' attenuating their backscattered powers. In the Neighbor Discovery process, tag k measures and reports to the reader the power received when tag i backscatters the readers' CW power P_t^{max} without attenuation (denoted as $P_{i,k}^C$). Upon receiving this information, the reader builds a power matrix $\boldsymbol{P^C} = [P_{i,k}^C]$ and an attenuation matrix γ=$[\gamma_{i,k}]$, where each element $\gamma_{i,k}$ represents the needed attenuation at the tag i, so that (when the reader transmits at P_t^{max}) the tag k receives the minimum required power $P_{r,min}^{tag}$, allowing the link between the two tags to exist. $\gamma_{i,k}$ is calculated by the reader as follows:

$$\gamma_{i,k} = \frac{P_{r,min}^{tag}}{P_{i,k}^C}, \tag{12}$$

assuming that $P_{i,k}^C \geq P_{r,min}^{tag}$ (i.e., the link exists) and therefore $\gamma_{i,k} \leq 1$). In Scenario C, if tag i is chosen to transmit to tag k, tag i will then be instructed by the reader to attenuate its backscattered power by the factor $\gamma_{i,k}$. Therefore, the received power at tag k will be the minimum required received power $P_{r,min}^{tag}$, while the power received at another tag m ($m \neq k$) can be calculated as $\gamma_{i,k}P_{i,m}^C$, where $P_{i,m}^C$ denotes the received power at tag m if tag i transmits without attenuating its backscattered power (according to the matrix $\boldsymbol{P^C}$). The tag scheduling problem for Scenario C can then be formulated as follows:

$$\text{Maximize: } F(\mathbf{x}, \mathbf{c}) = \sum x_i \; c_{(i,k)j} w_{(i,k)j},$$

$$\text{Subject to: C1: } \forall_i : x_i \in \{0,1\}, \quad \forall_{i,j,k} : c_{(i,k)j} \in \{0,1\},$$

$$\text{C2: } \forall_i : x_i \sum_{k,j} \left(c_{(i,k)j} \prod_{l \neq j} \bar{c}_{(i,k)l} \prod_{m \neq k} \bar{c}_{(i,m)q_m} \right) + \bar{x}_i \prod_{k,j} \bar{c}_{(i,k)j} = 1, k, m \in \Psi_i, \; j, l \in \{1, \ldots, n_{i,k}\}$$

$$\text{and } q_m \in \{1, \ldots, n_{i,m}\},$$

$$\text{C3: } \forall_{i,k,j} : g\left[c_{(i,k)j}, \sum_{m \neq i} c_{(m,k)q_{m,k}} \right] = 1,$$

$$q_{m,k} \in \{1, \ldots, n_{m,k}\}$$

$$\text{C4: } \forall_{i,k,j} : g\left[c_{(i,k)j}, \; \bar{I}_2\left(P_{i,k}^C\right) \right] = 1,$$

$$j \in \{1, \ldots, n_{i,k}\},$$

$$\text{C5: } \forall_{i,k} c_{(i,k)j} = 0 \text{ if } \frac{P_{r,min}^{tag}}{\sum_{l \neq i} \sum_{m,q} c_{(l,m)q} \gamma_{l,m} P_{l,k}^C} \leq \eta, \; j \in \{1, \ldots, n_{i,k}\}, q \in \{1, \ldots, n_{l,m}\}, \tag{13}$$

where the function $g(x, y) = x\bar{y} + \bar{x}$ expresses the constraint that y cannot occur if x occurs. $I_2(P_{i,k})$ is an indicator function s.t. $I_2(P_{i,k}) = 1$ if $P_{i,k} \geq P_{r,min}^{tag}$, and otherwise $I_2(P_{i,k}) = 0$. Constraint C1 is similar to constraint C1 in the Scenario B problem. Constraint C2 is similar to constraint C3 in Scenario B (eq. (11)). Constraint C3 is similar to constraint C4 in Scenario B (eq. (11)). Constraint C4 represents that a message copy can be transmitted only when the maximum backscattering power of the tag suffices, so that the corresponding communication link exists. Constraint C5 represents the interference constraints that a message copy cannot be successfully received when the total received interference power results in SIR $< \eta$.

Algorithm 3 Routing Protocol for Scenario C

Inputs: T: message list that includes all the messages that have been chosen to transmit.
Step 0: The reader transmits at its maximum power P_t^{max} and queries individual tags for newly generated messages. Based on the measurement of received backscattered power on each tag, the reader obtains $\mathbf{P^C}$ and γ. $T = \{\}$.
Step 1: Assign weights to the pending messages.
Step 2: Sort all the messages in a descending order of weights.
Step 3: Add the message with the largest weight to T.
Step 4: Check the next message on the weight-sorted list. If that message does not violate the constraints C1-C5 of (13) with the transmissions in set T, add it to set T. Otherwise it is rejected. Proceeds sequentially to the next message with the next largest weight until all the messages are checked.
Step 5: The reader sequentially checks each of the other copies of all the messages not selected for transmission, and then each of the copies of messages which are already being selected for transmission (starting from the shortest path to the longest paths), to see if they could still be transmitted without affecting the transmissions of the selected messages.
Step 6: Once a message or its copy reaches the message's destination, all the other copies of this message are erased from the nodes.

The formulated problem (13) is an Integer Programming problem with nonlinear constraints, which can be solved by greedy algorithm similar to that for Scenario A. Similar to Scenario B, this algorithm can be further improved if nodes that overhear a transmitted message are allowed to retain the message copy and try to route it on a non-preferred path. We summarize the steps of the protocol in Algorithm 3.

Considering the same example presented in Section VII-A, we obtain the values of $\mathbf{P^C} = [P_{i,k}^C]$ (the power received at tag k when tag i backscatters the readers' CW power P_t^{max} without attenuation) and $\gamma = [\gamma_{i,k}]$ (the needed attenuation coefficient of the tag i for the link from tag i to tag k to exist) as shown in Table 2. By solving the MINLP problem presented above and then sequentially checking if transmissions on non-preferred paths can still be sent, we obtain the optimal values of: ${c_{(2,9)1}}^* = 1$, ${c_{(3,8)1}}^* = 1$, ${c_{(4,7)1}}^* = 1$, ${c_{(5,10)1}}^* = 1$, ${c_{(10,1)1}}^* = 1$, ${c_{(6,5)1}}^* = 1$, ${c_{(8,3)1}}^* = 1$, ${c_{(9,6)1}}^* = 1$, and $\mathbf{x}^* = [0, 1, 1, 1, 1, 1, 0, 1, 1, 1]$. It shows that by attenuating backscattering powers, the network throughput (i.e., the number of concurrent transmissions) is improved from 5 (in Scenario B) to 8 (in Scenario C).

TABLE 2. The values of $P^{C}_{i,k}$ in dBm (the first value in each entry) and $\gamma_{i,k}$ (the second value in each entry); row indices indicate the transmitting tags, while the column indices indicate the receiving tags. Note that when $P^{C}_{i,k} < -20$ dBm or when $\gamma_{i,k} > 1$, the link from tag i to tag j cannot exist. available links are indicated by entries in bold font.

	1	2	3	4	5	6	7	8	9	10
1	-∞	-21.7, 1.5	-26.7, 4.6	-29.2, 8.4	**-18.0, 0.6**	-21.9, 1.6	-32.2, 16.5	-28.6, 7.3	**-15.2, 0.3**	**-16.5, 0.5**
2	**-13.6, 0.2**	-∞	**-16.1, 0.4**	**-17.1, 0.5**	**-15.1, 0.3**	**-1.8, 0.02**	-21.2, 1.3	**-18.1, 0.7**	**-8.2, 0.07**	**-13.8, 0.2**
3	-25.6, 3.6	-23.1, 2.0	-∞	-28.2, 6.6	-23.2, 2.1	-21.3, 1.3	-30.3, 10.7	**-14.0, 0.2**	-23.8, 2.4	-22.9, 2.0
4	-24.6, 2.9	-20.5, 1.1	-24.6, 2.9	-∞	-25.6, 3.6	-21.4, 1.4	**-16.8, 0.5**	-25.0, 3.2	-23.0, 2.0	-25.0, 3.2
5	**-18.7, 0.7**	-23.9, 2.5	-25.0, 3.2	-30.9; 12.4	-∞	-23.0, 2.0	-33.5, 22.2	-27.6, 5.7	**-19.9, 0.98**	**-7.1, 0.05**
6	**-14.8, 0.3**	**-2.8, 0.02**	**-15.2, 0.3**	**-18.9, 0.8**	**-15.1, 0.3**	-∞	-22.6, 1.8	**-17.8, 0.6**	**-9.6, 0.6**	**-13.7, 0.2**
7	-32.9, 19.4	-30.0, 10.0	-32.1, 16.2	-22.1, 1.6	-33.5, 22.2	-30.4, 11.0	-∞	-32.0, 15.9	-31.7, 14.7	-33.1, 20.2
8	-28.6, 7.2	-26.1, 4.1	**-15.0, 0.3**	-29.6, 9.1	-26.8, 4.8	-24.8, 3.0	-31.2, 13.3	-∞	-27.1, 5.1	-26.6, 4.6
9	**-12.3, 0.2**	**-13.4, 0.2**	-22.1, 1.6	-24.8, 3.0	**-16.4, 0.4**	**-13.8, 0.2**	-28.1, 6.5	-24.3, 2.7	-∞	**-14.2, 0.3**
10	**-16.4, 0.4**	-21.8, 1.5	-23.9, 2.5	-29.6, 9.0	**-6.3, 0.04**	-20.7, 1.2	-32.2, 16.8	-26.5, 4.5	**-16.9, 0.5**	-∞

VIII. REGION PARTITION SCHEME FOR LARGE SCALE T2T NETWORKS

In this section, we propose a scheme — a region partition scheme — so that the proposed protocols can be executed efficiently for large-scale networks. The superiority of this scheme is in its computation time that increases linearly with the number of tags, rather than exponentially (which is the case for most existing protocols). The main idea of the proposed scheme is that we partition the network into small regions with approximately the same number of tags in each region, and then use the methods proposed in Sections VI and VII to solve for each region, so that the execution complexity is significantly reduced, resulting in total complexity scaling linearly with the number of regions (and, thus, in essence with the number of tags).

As the proposed partition scheme divides the global problem into separate partial problems, the scheme needs to resolve two challenges to yield a global solution: (1) since transmissions are solved in each region separately, there might exist inter-region transmissions (i.e., a transmission that is sent from a tag in one region and received from a tag in another region) that need to be taken reconciled, and (2) the separate solutions may result in "incompatible" transmission in different regions (i.e., a transmission selected from one region that interferes with transmissions in other regions).

To address the above issues, after the network is divided into regions, each region G is extended with a "boundary area" G' in which tags from the neighboring regions are included, if such tags can receive or be interfered by tags in G. To fully consider all possible transmissions in the entire area including inter-region transmissions, we then run the transmission algorithm in each individual region $G \cup G'$ (termed as an "extend region") separately. Note that for each extended region $G \cup G'$, we consider all transmissions from tags in region G to tags in the extended region $G \cup G'$, so that: (1) inter-region transmissions can are considered even with region partition, and (2) each transmission is only considered once globally. To be more specific, although an inter-region transmission involves tags in two different regions, it is only considered in the region of the transmitting tag. To resolve inconsistencies of the individual solutions (i.e., transmissions from the boundary areas that may conflict with the transmission assignments in the G region), a simple algorithm is employed which rejects the possible inconsistencies of the tags in the boundary areas G's for each region. This algorithm may end up selecting smaller than the maximum number of transmissions, but as shown in Section IX, the penalty in global throughput is small.

The way to identify boundary areas is different for each scenario and is described next. In general, for a region G, we consider the set of all the tags that can be interfered by tags in a neighboring region (according to the collision map) as to create the boundary area G'. In scenario A, tags in a boundary area can be identified through the Neighbor Discovery process. As described in Section VI, the reader constructs a connection map and a collision map, which is used to select the boundary areas. In scenarios B and C, tags are capable of measuring their received powers. In scenario B, the information of available transmission links is provided by matrix $\mathbf{P^B}$ which includes needed transmit power of the reader for links between two tags to exist. Since in scenario B the transmit power of the reader P_t is a variable that needs to be optimized, the transmission links (and therefore the tags in boundary areas) vary with the choice of P_t. For scenario C, on the other hand, the reader always transmits at its maximum power $P_t^{max} = 1$ Watt. Based on the matrix $\mathbf{P^C}$, the reader can identify tags in the boundary areas.

Since transmissions to tags in a region may receive interference from tags in other regions (when it's in the boundary areas of those regions), after transmissions are selected for each extended region (using the previously described algorithms), we then check the compatibility of solutions among different regions. To do that, we first identify all tags that are in at least one boundary area (these tags are referred to as "boundary-area tags") and their corresponding regions. For example, a tag i in G_1 that can receive from at least one tag in G_2 and at least one tag in G_3 can be identified as a "boundary-area tag" in the boundary areas G'_2 and G'_3. Then for each boundary-area tag that is selected to receive a transmission, we evaluate if the selected transmissions in those corresponding regions would interfere. If so, the transmission to that boundary-area tag will be removed

TABLE 3. The simulation parameters.

Parameter	Notation	Value
operational wavelength	λ	1 m
backscattering loss	K	-10 dB
Maximum transmit power of the reader	P_{max}	1 Watt
required minimum reception signal at tags	$P_{r,min}^{tag}$	-20 dBm

from the selected transmission set. The compatibility check is based on collision maps in scenario A. For example, when the aforementioned tag i in the boundary areas G_2' and G_3' is selected to receive from tag j, we check all the selected transmitting tags in the extended regions $G_2 \cup G_2'$ and $G_3 \cup G_3'$. If a transmitting tag k ($k \neq j$) in G_2 or G_3 can interfere with the receiving tag i, that transmission to tag i will not be successful and therefore needs to be removed from the global solution set. In scenarios B and C, due to additional hardware capability, we evaluate SIR at each receiving tag. For example, when tag m in the boundary areas G_2' and G_3' is selected to receive in transmission t, we consider the accumulated interference from all selected transmissions in the extended regions $G_2 \cup G_2'$ and $G_3 \cup G_3'$. If the tag m receives too much interference (i.e., $SIR < \eta$), that corresponding transmission t needs to be inhibited.

IX. SIMULATION RESULTS

In this section, we evaluate our T2T protocols by MATLAB simulation of the proposed algorithms for all the three scenarios, using a computer with an Intel Core i5-7500 CPU @ 3.40 GHz processor and a 16.00 GB RAM. In Section IX-A, we evaluate the impacts of the setting levels of reader power P_L and P_H on network capacities in Scenario A. We also investigate the discrepancy between the predicted throughput of the routing protocol and the actual throughput. Then in Section IX-B and C, we apply the proposed protocols to an example of a large-scale network with 10,000 tags. We evaluate network capacity and time complexity for each scenario, as well as demonstrate the reduction in time complexity of the region partition scheme proposed in Section VIII.

In the MATLAB implementation, tags are uniformly distributed within a circular area with a radius of 5 m, and the reader is located at the center of this area. For the region partition scheme, we divide the circular area into 10 equal sectors, and then further divide each sector into 10 regions, so that the areas of all the regions are the same, and all regions, thus, have about the same number of tags. Since the tags are uniformly deployed in the area, there are approximately 100 tags in each divided region. The parameter settings are listed in Table 3.

A. T2T ROUTING PROTOCOL FOR SCENARIO A

1) DATA THROUGHPUT VS. P_L FOR DIFFERENT TAG DENSITY

The T2T routing protocol for Scenario A uses a "margin" in link discovery to (at least partially) compensate for the additive nature of interference. More specifically, two reader's CW power levels are defined, P_L and P_H, that allows creating this "margin" of power. As one could anticipate, settings of these power levels have a critical effect on the performance of the Scenario A routing protocol, which we evaluate next for various tag densities.

Another aspect of the routing algorithm for Scenario A that is important to understand is the discrepancy between the predicted throughput of the routing protocol, and the actual throughput. More specifically, in the proposed algorithm for Scenario A, for each transmission, only the interference from one neighbor tag is considered (as determined by the interference discovery at reader's CW power of P_H), rather than the total cumulative interference from all neighbor tags. Although the margin of $P_H - P_L$ to somewhat compensates for the lack of considering the cumulative interference, this margin may not suffice in all situations. Therefore, we evaluate how much the throughput calculated by our algorithm for Scenario A diverges from the actual throughput that could be achieved if transmissions were disabled based on the sum of all interferences. More specifically, we compare the "predicted throughput" (i.e., the maximum number of concurrent transmissions as calculated by the proposed routing algorithm, which ignores cumulative interference) with the "actual throughput" (i.e., the maximum number of concurrent transmissions as evaluated by simulation, which considers all the combined interferences),[9] both at the reader's power of P_L. Here, the SIR threshold η is set to 0 dB.[10]

We set the reader's CW power for interfering link discovery at P_H= 1 W. (This setting maximizes the interfering link discovery, although the general conclusions in this subsection hold for other settings of P_H as well.) Then we investigate the impact of the reader's CW power for link discovery, P_L, on the data throughput (i.e., the number of concurrent transmissions), when P_L varies from 0.2 Watt to 1 Watt. Fig. 5 shows the simulation results for different tag densities, μ. We assume that each tag which has available transmission links (i.e., which has sufficient backscattering power to reach another tag) has at least one message to transmit. We used the algorithm of Scenario A from Section VI to determine the set of transmitting tags.

As it is intuitive, Fig. 5 shows that the actual throughput is generally less than the predicted throughput. The difference between both throughputs increases as P_L increases. It is also shown that, in general, for each tag density, there is an optimal power P_L that maximizes the actual throughput. For the small density of 2 $/m^2$, the maximum is not evident in the figure, as it would occur at $P_L > 1$ W (which is an infeasible setting as P_H= 1 W and $P_H \geq P_L$). In general, as the value of P_L increases, the actual average network throughput first increases and then decreases. This can be explained by the fact that for small values of P_L, the power of CW is insufficient to create many links. However, when

9. Note that this is different than maximum network throughput.

10. Which would be the case, for example, when the tags use CDMA modulation [77].

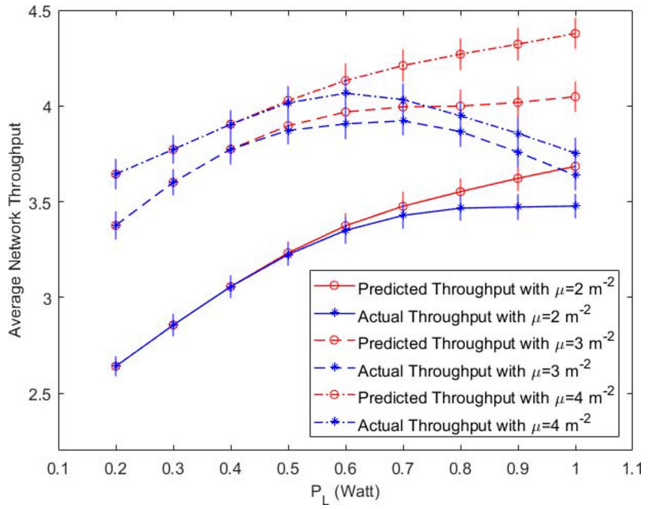

FIGURE 5. Actual/Predicted data throughput vs. P_L for different tag density. 95% confidence intervals are shown.

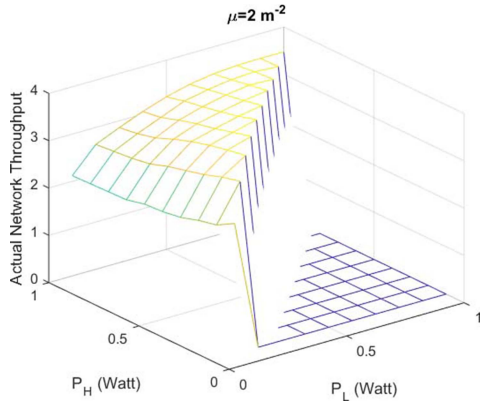

FIGURE 6. Actual Throughput vs. P_H vs. P_L ($\mu = 2/m^2$).

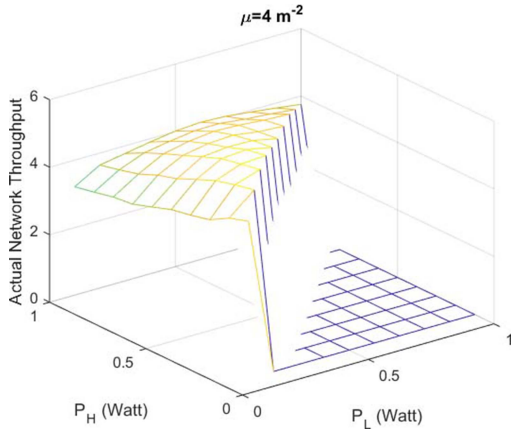

FIGURE 7. Actual Throughput vs. P_H vs. P_L ($\mu = 4/m^2$).

P_L is too high, the interference from multiple tags may add together to prevent a tag from receiving, although each interference by itself does not have enough power to take the link down. In fact, this is exactly why we introduced the two levels of CW power (P_H for interference discovery and $P_L$for link discovery), by realizing that interference from multiple sources can disrupt a link.

From Fig. 5, we also see that the optimal CW power P_L tends to decrease as the density μ increases, since as μ increases the inter-tag distances are reduced, increasing the inter-tag interferences. In summary, the above discussion of Fig. 5 demonstrates that judicious selection of the P_L is critical for achieving maximal capacity of the routing algorithm, especially for large tag densities. As the tag density would typically be unknown to the reader in most practical situations, one possible approach is for the reader to progressively increase the value of P_L, while observing the performance, thus allowing the reader to arrive at a near-optimal setting for the value of P_L.

2) SETTING P_H VS. P_L TO MAXIMIZE THROUGHPUT

For maximal throughput, the setting of the powers, P_L and P_H should be optimized. We also note that, although in the previous section for demonstration purposes we set P_H to 1 Watt, so as to discover most interfering links, however, for such high P_H the transmission links might be "overprotected". In other words, since P_L is used for transmission, there might be transmissions that do not interfere, but were inhibited, since they were evaluated under a too large P_H. Therefore, we investigate now the joint impact of both P_H and P_L on the actual data throughput. All the simulation parameters are set as in the previous section, except that $0.1[W] \leq P_L \leq P_H \leq 1[W]$.

As shown in Fig. 5, for $P_L \leq P_H$, when P_L is fixed, the average network throughput monotonically decreases as P_H increases. This decrease is due to the fact that available links are determined by P_L, while increasing P_H disables more links. However, the number of "overprotected" links increases as P_H increases. In Fig. 6, with a larger tag density, when P_L is set in a certain range (e.g., when $P_L = 0.3$ Watt), the average network throughput first increases and then decreases as P_H increases. This increase in the throughput is due to the fact that when P_H is too small, there exist transmissions that actually cause interference, but are not identified as such (due to too small P_H), thus resulting in a reduced network throughput. From Fig. 7, it is evident that the impact of P_L on the average network throughput is generally larger than that of P_H, but that the impact of P_H increases as the tag density increases. This latter trend is due to the smaller inter-tag distances at low tag density, so that there is more interference (and more interference detected at higher P_H level) that more significantly affects the data throughput.

The above discussion of Figs. 6 and 7 demonstrates again that judicious selection of the values of P_L and P_H is critical for achieving maximal capacity of the routing algorithm for Scenario A, especially for large tag densities. As mentioned above, in practical situations, the reader could progressively increase the value of $P_L$and P_H (likely in some discrete increments), while observing the performance, thus allowing the reader to arrive at its near-optimal setting.

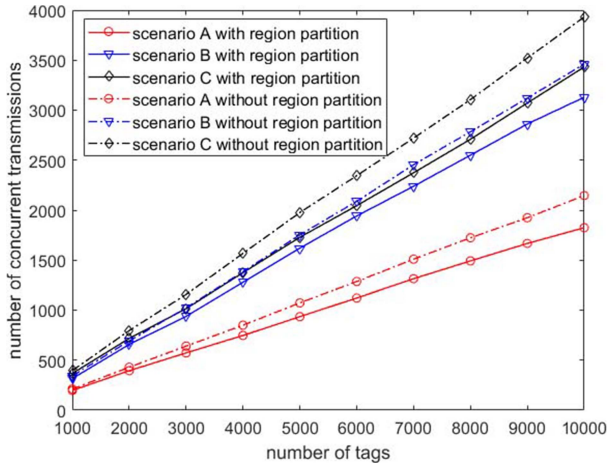

FIGURE 8. Number of tags vs. network capacity.

B. NETWORK CAPACITY

In this section, we evaluate the network capacity using the proposed routing protocols in the three scenarios, with the goal of understanding how much the extra hardware capabilities of the tags (i.e., the power measurement and the transmission attenuation) contribute to the throughput improvement. We also demonstrate the notable reduction of the time complexity of the algorithms through our region partition scheme, as to show that with a small penalty in capacity, our region partition scheme significantly reduces the computation time needed for the large-scale networks. For Scenario A, we set $P_H = 1$ Watt and $P_L = 0.75$ Watt. For Scenario B, we search the transmit power of the reader in 20 discrete values, starting from 0.24 Watt with increments of 0.04 Watt. For tags in Scenario C, the reader always operates at the maximal power level $P_R = 1$ Watt. As the aim of this simulation is to evaluate the number of concurrent transmissions, we assume that there is always a message available to be sent on every existing communication link.

Fig. 8 shows that the throughput of all the three scenarios (with and without the region partition scheme) monotonically increases with the number of tags. The number of tags varies from 1000 to 10000, with each region containing 1000 tags. The data throughput of tags in Scenario C is larger than that in Scenario B, because of the minimized interference of tags in Scenario C when tags are able to attenuate their backscattered power. The data throughput of Scenario B is larger than tags in Scenario A, because the values of P_H and P_L in Scenario A are static and thus not necessarily optimal for a particular setting. Indeed, since in Scenario A the actual performance highly depends on the optimality of the choices of P_H and P_L, the network capacity in Scenario A would typically be much lower than that in Scenario B. However, if P_H and P_L could be set to be optimal, the performance of Scenario A would be close to that of Scenario B. The throughputs obtained by schemes with region partition are always slightly lower than the schemes without region partition, due to the small penalty

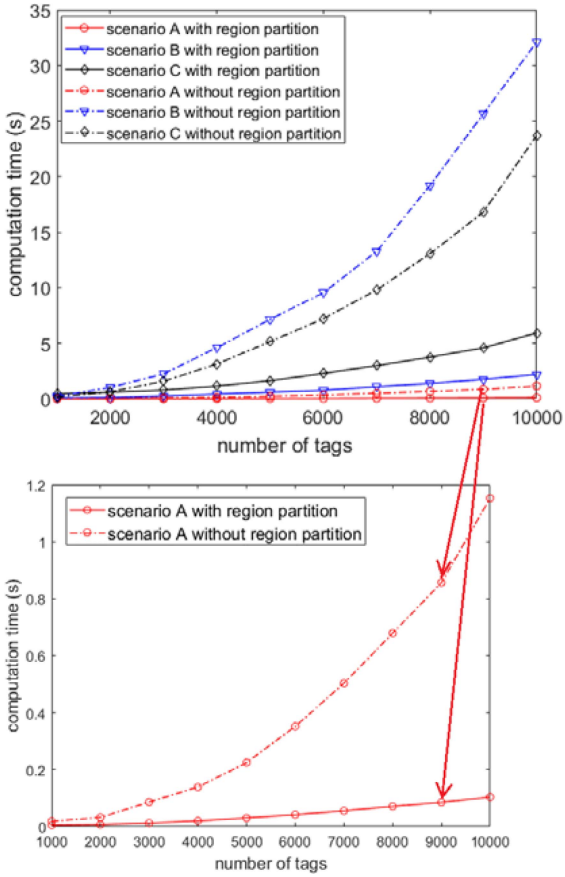

FIGURE 9. Number of Tags vs. Computation Time.

of the region partition scheme; i.e., the partitioning the globally optimal solution results in a small degradation, but with substantial complexity reduction.

C. COMPUTATION TIME COMPLEXITY

The complexity of the routing protocols in a large-scale network is a critical factor for real-time applications. In this section, we demonstrate that our proposed scheme with region partition has a significant improvement in large-scale network settings. In general, as the number of tags increases, the time complexity of a routing algorithm increases exponentially. However, with our region partition scheme, as the number of tags increases, only the number of regions increases, but the time to solve each region remains constant. Thus, increasing the number of tags leads only to the linear processing time increase.

For demonstration purpose in this section, we evaluated the computation time of a MATLAB implementation of the proposed algorithms for all the three scenarios, using a computer with an Intel Core i5-7500 CPU @ 3.40 GHz processor and a 16.00 GB RAM.

Fig. 9 shows that the computation time of Scenario A is the shortest because of the relatively simpler formulation of the optimization problem. The computation time of Scenario B is the longest, because (as opposed to Scenario C) Scenario B

TABLE 4. Neighbor table of the example.

	(a_1, b_1)	(a_2, b_2)	(a_3, b_3)	(a_4, b_4)	(a_5, b_5)	(a_6, b_6)	(a_7, b_7)	(a_8, b_8)
tag 1	N/A	(1,1)	(0,1)	(0,0)	(0,0)	(0,0)	(0,0)	(0,0)
tag 2	(1,1)	N/A	(0,1)	(0,0)	(1,1)	(0,1)	(0,0)	(0,0)
tag 3	(1,1)	(0,1)	N/A	(0,1)	(0,0)	(0,0)	(0,0)	(1,1)
tag 4	(0,0)	(0,0)	(1,1)	N/A	(0,1)	(0,0)	(1,1)	(0,0)
tag 5	(0,0)	(1,1)	(0,1)	(1,1)	N/A	(0,1)	(0,1)	(0,0)
tag 6	(0,0)	(1,1)	(0,0)	(0,0)	(1,1)	N/A	(0,0)	(0,0)
tag 7	(0,0)	(0,0)	(0,0)	(1,1)	(0,0)	(0,0)	N/A	(0,0)
tag 8	(0,0)	(0,0)	(1,1)	(0,0)	(0,0)	(0,0)	(0,0)	N/A

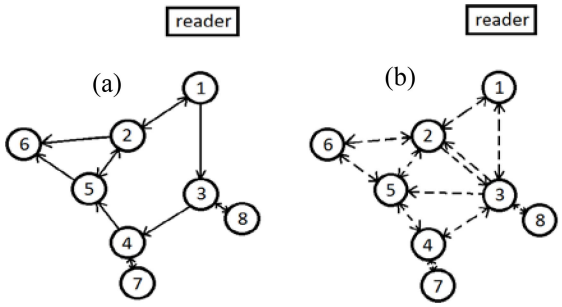

FIGURE 10. (a) Connection map; (b) Collision map (link from *i* to *j* indicates that *i* cannot transmit, while *j* is receiving).

TABLE 5. Routing table of the example.

from\to	tag 1	tag 2	tag 3	tag 4	tag 5	tag 6	tag 7	tag 8
tag 1	N/A	1-2; 1-3-4 -5-2	1-3	1-3-4	1-2-5 ; 1-3-4 -5	1-2-6;1-2-5-6; 1-3-4-5-6	1-3-4 -7	1-3-8
tag 2	2-1	N/A	2-1-3	2-1-3 -4	2-5; 2-1-3-4-5	2-6; 2-5-6	2-1-3 -4-7	2-1-3 -8
tag 3	3-4-5 -2-1	3-4-5 -2	N/A	3-4	3-4-5	3-4-5-6; 3-4-5-2-6	3-4-7	3-8
tag 4	4-5-2 -1	4-5-2	4-5-2-1 -3	N/A	4-5	4-5-6;4-5 -2-6	4-7	4-5-2 -1-3-8
tag 5	5-2-1	5-2	5-2-1-3	5-2-1 -3-4	N/A	5-6;5-2 -6	5-2-1 -3-4-7	5-2-1 -3-8
tag 6	Can't reach	Can't reach	Can't reach	Can't reach	Can't reach	N/A	Can't reach	Can't reach
tag 7	7-4-5 -2-1	7-4-5 -2	7-4-5-2 -1-3	7-4	7-4-2	7-4-5-6; 7-4-5-2-6	N/A	7-4-5 -2-1-3-8
tag 8	8-3-4-5-2-1	8-3-4 -5-2	8-3	8-3-4	8-3-4 -5	8-3-4-5-6; 8-3-4-5-2-6	8-3-4 -7	N/A

requires optimization of the transmission power. Combining the results in Figs. 8 and 9, we can see that in general the region partitioning slightly reduces the network capacity, but impressively improves time efficiency. In conclusion, the region partitioning scheme is an excellent approach to design practical routing algorithms for large-scale T2T networks.

The simulation results of our evaluations of the three different scenarios allow us to make the following recommendations: for middle-to-large size networks the extra power measurement capability of Scenario B and C leads to a significant improvement in throughput as opposed to Scenario A, especially for large-scale networks. The backscattering attenuation of Scenario C adds additional worthwhile improvement in capacity for large-scale networks. These improvements should be considered sufficient incentives to invest in the extra hardware capabilities of the tags (i.e., power measurement and backscattering attenuation). The implementation of the region partition scheme is essential for large-scale networks in any of the three schemes, but definitely for Scenarios B and C.

X. CONCLUSION AND FUTURE WORK

In this paper, we presented a novel multi-hop passive RFID T2T network model named *NeTa*, which incorporates the turbo backscattering operation for multi-hop routing of messages. The proposed scheme considerably enhances the network coverage through multi-hop routing, and significantly increases the overall network throughput through distributed routing. Due to the asymmetry of communication links and interferences in such a network, existing routing protocols cannot be used. To address this shortcoming, we proposed a routing protocol to identify tags and their multiple-hop uplink routing. Then considering three types of passive RFID tags with different capabilities (i.e., received power measurements and transmission power attenuation), we proposed three corresponding routing protocols to schedule transmissions, as to maximize the overall network throughput. Utilizing a greedy algorithm and a region partition scheme, our proposed algorithm can coordinate transmissions to increase network capacity in large-scale networks, with a low-complexity computation time which has a linear relationship with the number of tags.

In general, the results of this research will allow designers of this new breed of multi-hop battery-less tag networks to optimally select the needed tag capabilities and to optimally set the parameters of the routing protocols depending on the network topologies.

The paper addressed only networks with stationary tags. Extension of our work to mobile environment will add an interesting dimension to future applicability of the work.

APPENDIX
SIMPLE EXAMPLE OF ROUTING PROTOCOLS FOR SIMPLE TAGS – SCENARIO A

We consider here a simple example and follow the corresponding routing process as to demonstrate the steps of the routing protocol. The purpose of the example is to further clarify how the algorithm in Section VI-B operates. Assuming a simple T2T network consisting of a reader and 8 tags. The complete neighbor table obtained by the Neighbor Discovery process is shown as Table 4. In Table 4, a_i in a particular row of tag j indicates whether a transmission link from tag i to the tag j exists when the reader transmits at power P_L, and b_i indicates whether an interfering link from tag i to tag j exists[11] when the reader transmits at

11. An interfering link from tag i to tag j indicates that i cannot transmit, while j is receiving from another tag.

power P_H. a_i and b_i are both binary variables: "1" represents that a link/interference exists and "0" represents that a link/interference does not exist.

In this example, we assume that there are 5 message copies that need to be transmitted on their preferred routing paths, as follows:

- c_{11}: from tag 1 to tag 3, with priority parameter $p_{11} = 1$, having no delay ($d_{11} = 0$)
- c_{12}: from tag 1 to tag 4, with priority parameter $p_{12} = 2$, having 1 time slot of delay ($d_{12} = 1$)
- c_{41}: from tag 4 to tag 5, with priority parameter $p_{41} = 3$, having no delay ($d_{41} = 0$)
- c_{51}: from tag 5 to tag 1, with priority parameter $p_{51} = 3$, having no delay ($d_{51} = 0$)
- c_{71}: from tag 7 to tag 4, with priority parameter $p_{71} = 3$, having 2 time slots of delay ($d_{71} = 2$)

From Table 4, the reader can construct a connection map and a collision map as shown in Fig. 10 (a) and (b), respectively. From the connection map in Fig. 10 (a), the reader constructs a complete routing table for every link as shown in Table 5. In this example, the shortest routing path between each pair of tags is selected as the preferred routing path.

We assume that there already also exist two message copies on non-preferred routing paths:

- c_{71}^{copy}: A copy of the message c_{71} from tag 2 to tag 4.
- c_{11}^{copy}: A copy of the message c_{11} from tag 8 to tag 3.

The weights of messages on the preferred routing paths, assuming $\alpha = 0.2$ and $\beta = 0.3$, are:

$$\begin{aligned} w_{11} &= p_{11}(1 + d_{11}\alpha)(1 + h_{11}\beta) = 1.3; \\ w_{12} &= p_{12}(1+d_{12}\alpha)(1 + h_{12}\beta) = 3.12, \\ w_{41} &= p_{41}(1 + d_{41}\alpha)(1 + h_{41}\beta) = 3.9; \\ w_{51} &= p_{51}(1+d_{51}\alpha)(1 + h_{51}\beta) = 4.8, \\ w_{71} &= p_{71}(1+d_{71}\alpha)(1 + h_{71}\beta) = 5.4. \end{aligned}$$

The C2 constraints can be expressed as below:

- *Tag 1:* $x_1\ (c_{11}\ \bar{c}_{12} + \bar{c}_{11}\ c_{12}\ ) + \bar{x}_1\bar{c}_{11}\bar{c}_{12} = 1$,
- *Tag 2:* $\bar{x}_2 = 1$,
- *Tag 3:* $\bar{x}_3 = 1$,
- *Tag 4:* $x_4 c_{41} + \bar{x}_4\bar{c}_{41} = 1$,
- *Tag 5:* $x_5 c_{51} + \bar{x}_5\bar{c}_{51} = 1$,
- *Tag 6:* $\bar{x}_6 = 1$,
- *Tag 7:* $x_7 c_{71} + \bar{x}_7\bar{c}_{71} = 1$.

Note that the constraint C2 does not apply to the state of tag 8, which has only a message copy on non-preferred routes.

Based on the neighbor table which contains information on all the interfering nodes, the constraint C3 can be written as:

$$\begin{aligned} c_{11} &: g(c_{11}, x_2 + x_4 + x_8) = 1; \\ c_{12} &: g(c_{11}, x_2 + x_4 + x_8) = 1; \\ c_{41} &: g(c_{41}, x_2 + x_3 + x_6) = 1, \\ c_{51} &: g(c_{51}, x_1 + x_3 + x_6) = 1; \\ c_{71} &: g(c_{71}, x_3 + x_5) = 1. \end{aligned}$$

By solving this binary optimization problem of eq. (7), the optimal values are:

$$\begin{aligned} \mathbf{c}^* &= \{c_{11}^*,\ c_{12}^*,\ c_{41}^*,\ c_{51}^*,\ c_{71}^*\} = [0, 0, 1, 0, 1]; \\ \mathbf{x}^* &= [x_1^*,\ x_2^*,\ x_3^*,\ x_4^*,\ x_5^*,\ x_6^*,\ x_7^*,\ x_8^*] \\ &= [0, 0, 0, 1, 0, 0, 1, 0]. \end{aligned}$$

The obtained scheduling shows that 2 messages will be transmitted in this cycle.

Thereafter, the reader sequentially checks each of the other message copies if they could still be transmitted. The reader should first check for all the messages not selected for transmission (starting from the shortest path to the longest path). Then, similarly, the reader checks the copies of messages that already have a copy being transmitted (starting from the shortest path to longest paths), until all the copies have been checked. Therefore, in this example, we check the message copies in the following order: (1) c_{11}^{copy}: cannot be transmitted since tag 4 is transmitting, and (2) c_{71}^{copy}: can be transmitted. Once a message reaches its destination, its copies are erased from all the non-destination nodes.

REFERENCES

[1] Z. Shen, A. Athalye, and P. M. Djurić, "Phase cancellation in backscatter-based tag-to-tag communication systems," *IEEE Internet Things J.*, vol. 3, no. 6, pp. 959–970, Dec. 2016.

[2] D. De Donno, L. Catarinucci, and L. Tarricone, "A battery-assisted sensor-enhanced RFID tag enabling heterogeneous wireless sensor networks," *IEEE Sensors J.*, vol. 14, no. 4, pp. 1048–1055, Apr. 2014.

[3] P. V. Nikitin, S. Ramamurthy, R. Martinez, and K. V. S. Rao, "Passive tag-to-tag communication," in *Proc. IEEE Int. Conf. RFID (RFID)*, Orlando, FL, USA, Apr. 2012, pp. 177–184.

[4] C. Liu and Z. J. Haas, "Routing protocol design in tag-to-tag networks with capability-enhanced passive tags," in *Proc. IEEE 28th Annu. Int. Symp. Pers. Indoor Mobile Radio Commun. (PIMRC)*, Montreal, QC, Canada, 2017, pp. 1–6.

[5] C. Liu and Z. J. Haas, "Multi-hop routing protocols for RFID systems with tag-to-tag communication," in *Proc. IEEE Military Commun. Conf. (MILCOM)*, Baltimore, MD, USA, 2017, pp. 563–568.

[6] H. Nakamoto *et al.*, "A passive UHF RF identification CMOS tag IC using ferroelectric RAM in 0.35- μm technology," *IEEE J. Solid-State Circuits*, vol. 42, no. 1, pp. 101–110, Jan. 2007.

[7] J. Lee, N. D. Phan, D. H. Vo, and V. Duong, "A fully integrated EPC Gen-2 UHF-band passive tag IC using an efficient power management technique," *IEEE Trans. Ind. Electron.*, vol. 61, no. 6, pp. 2922–2932, Jun. 2014.

[8] H. Liu, M. Hua, C. Peng, and J. Ciou, "A novel battery-assisted class-1 generation-2 RF identification tag design," *IEEE Trans. Microw. Theory Techn.*, vol. 57, no. 5, pp. 1388–1397, May 2009.

[9] Y. Du, Y. Zhuang, X. Li, W. Liu, Z. Li, and Z. Qi, "An ultra low-power solution for EEPROM in passive UHF RFID tag IC with a novel read circuit and a time-divided charge pump," *IEEE Trans. Circuits Syst. I, Reg. Papers*, vol. 60, no. 8, pp. 2177–2186, Aug. 2013.

[10] V. Duong, N. X. Hieu, H. Lee, and J. Lee, "A battery-assisted passive EPC Gen-2 RFID sensor tag IC with efficient battery power management and RF energy harvesting," *IEEE Trans. Ind. Electron.*, vol. 63, no. 11, pp. 7112–7123, Nov. 2016.

[11] J. Yin *et al.*, "A system-on-chip EPC Gen-2 passive UHF RFID tag with embedded temperature sensor," *IEEE J. Solid-State Circuits*, vol. 45, no. 11, pp. 2404–2420, Nov. 2010.

[12] K. Kapucu and C. Dehollain, "Base-station design for passive UHF RFID tags with pulse-width modulated backscattering," in *Proc. 10th Conf. Ph.D. Res. Microelectron. Electron. (PRIME)*, Grenoble, France, 2014, pp. 1–4.

[13] Q. Zhang, M. Crisp, I. H. White, and R. V. Penty, "Power margin reduction in linear passive UHF RFID tag arrays," in *Proc. IEEE RFID Technol. Appl. Conf. (RFID-TA)*, Tampere, Finland, 2014, pp. 306–311.

[14] K. Kapucu and C. Dehollain, "A passive UHF RFID system with a low-power capacitive sensor interface," in *Proc. IEEE RFID Technol. Appl. Conf. (RFID-TA)*, Tampere, Finland, 2014, pp. 301–305.

[15] Y. Zheng and M. Li, "Fast tag searching protocol for large-scale RFID systems," *IEEE/ACM Trans. Netw.*, vol. 21, no. 3, pp. 924–934, Jun. 2013.

[16] H. Yue, C. Zhang, M. Pan, Y. G. Fang, and S. Chen, "A time-efficient information collection protocol for large-scale RFID systems," in *Proc. IEEE INFOCOM*, Orlando, FL, USA, 2012, pp. 2158–2166.

[17] S. W. Wang, W. H. Chen, C. S. Ong, L. Liu, and Y. W. Chuang, "RFID application in hospitals: A case study on a demonstration RFID project in a Taiwan hospital," in *Proc. 39th Annu. Hawaii Int. Conf. Syst. Sci. (HICSS'06)*, Kauia, HI, USA, 2006, p. 184a.

[18] S. Dominikus, M. Aigner, and S. Kraxberger, "Passive RFID technology for the Internet of Things," in *Proc. Int. Conf. Internet Technol. Secured Trans.*, London, U.K., 2010, pp. 1–8.

[19] D. Fortin-Simard, K. Bouchard, S. Gaboury, B. Bouchard, and A. Bouzouane, "Accurate passive RFID localization system for smart homes," in *Proc. IEEE 3rd Int. Conf. Netw. Embedded Syst. Every Appl. (NESEA)*, Liverpool, U.K., 2012, pp. 1–8.

[20] S.-H. Baeg, J.-H. Park, J. Koh, K.-W. Park, and M.-H. Baeg, "Building a smart home environment for service robots based on RFID and sensor networks," in *Proc. Int. Conf. Control Autom. Syst.*, Seoul, South Korea, 2007, pp. 1078–1082.

[21] Y. Cui, Y. Yao, and G. Xu, "Research of ubiquitous power Internet of Things security authentication method based on CPK and RIFD," in *Proc. IEEE 4th Inf. Technol. Netw. Electron. Autom. Control Conf. (ITNEC)*, Chongqing, China, 2020, pp. 1519–1523.

[22] E. E. Tsiropoulou, J. Baras, S. Papavassiliou, and S. Sinha, "RFID-based smart parking management system," *Cyber Phys. Syst.*, vol. 3, pp. 22–41, Aug. 2017.

[23] L. Catarinucci, R. Colella, and L. Tarricone, "Integration of RFID and sensors for remote healthcare," in *Proc. 3rd Int. Symp. Appl. Sci. Biomed. Commun. Technol. (ISABEL)*, Rome, Italy, 2010, pp. 1–5.

[24] Y. Xiao, X. Shen, B. Sun, and L. Cai, "Security and privacy in RFID and applications in telemedicine," *IEEE Commun. Mag.*, vol. 44, no. 4, pp. 64–72, Apr. 2006.

[25] G. Oguntala *et al.*, "Design framework for unobtrusive patient location recognition using passive RFID and particle filtering," in *Proc. Internet Technol. Appl. (ITA)*, Wrexham, U.K., 2017, pp. 212–217.

[26] A. Naveen and A. Kushwaha, "Smart Forest Surveillance Unit (S.F.S)," in *Proc. 2nd Int. Conf. Intell. Comput. Instrum. Control Technol. (ICICICT)*, Kannur, India, 2019, pp. 714–717.

[27] A. Scalera *et al.*, "The PigWise project: A novel approach in livestock farming through synergistic performances monitoring at individual level," in *Proc. Sustain. Agriculture ICT Innovat.*, Turin, Italy, Jun. 2013, pp. 24–27.

[28] M. S. Khan, M. S. Islam, and H. Deng, "Design of a reconfigurable RFID sensing tag as a generic sensing platform toward the future Internet of Things," *IEEE Internet Things J.*, vol. 1, no. 4, pp. 300–310, Aug. 2014.

[29] G. Marrocco and C. Stefano, "Electromagnetic models for passive tag-to-tag communications," *IEEE Trans. Antennas Propag.*, vol. 60, no. 11, pp. 5381–5389, Nov. 2012.

[30] J. Ryoo, Y. Karimi, A. Athalye, M. Stanaćević, S. R. Das, and P. Djurić, "BARNET: Towards activity recognition using passive backscattering tag-to-tag network," in *Proc. 16th Annu. Int. Conf. Mobile Syst. Appl. Serv.*, 2018, pp. 414–427.

[31] M. Li, H. Xie, W. Wang, X. Li, C. Wang, and Y. Zhang, "An advanced anti-collision algorithm based on inter-tag communication mechanism in RFID-sensor network," in *Proc. IEEE 11th Int. Conf. Mobile Ad Hoc Sens. Syst.*, Philadelphia, PA, USA, 2014, pp. 618–623.

[32] Y. Chang and T. K. Shih, "RFID-Based intelligent parking management system with indoor positioning and dynamic tracking," in *Proc. 10th Int. Conf. Ubi Media Comput. Workshops (Ubi-Media)*, Pattaya, Thailand, 2017, pp. 1–8.

[33] J. Ryoo, J. Jian, A. Athalye, S. R. Das, and M. Stanaćević, "Design and evaluation of 'BTTN': A backscattering tag-to-tag network," *IEEE Internet Things J.*, vol. 5, no. 4, pp. 2844–2855, Aug. 2018.

[34] H. Niu and S. Jagannathan, "A cross layer routing scheme for passive RFID tag-to-tag communication," in *Proc. 39th Annu. IEEE Conf. Local Comput. Netw.*, Edmonton, AB, Canada, Sep. 2014, pp. 438–441.

[35] (Oct. 2014). *FCC Code of Federal Regulations, Title 47, Volume 1, Part 15, Sections 245–249. 47CFR15*. Accessed: Jul. 28, 2020. [Online]. Available: https://www.fcc.gov/wireless/bureau-divisions/technologies-systems-and-innovation-division/rules-regulations-title-47

[36] K. Cha, A. Ramachandran, S. Jagannathan, and D. Pommerenke, "Decentralized power control with implementation for RFID networks," in *Proc. 45th IEEE Conf. Decis. Control*, San Diego, CA, USA, 2006, pp. 1858–1863.

[37] S. Subedi, E. Pauls, and Y. D. Zhang, "Accurate localization and tracking of a passive RFID reader based on RSSI measurements," *IEEE J. Radio Freq. Identif.*, vol. 1, no. 2, pp. 144–154, Jun. 2017.

[38] S. Srikant and R. P. Mahapatra, "Read range of UHF passive RFID," *Int. J. Comput. Theory Eng.*, vol. 2, no. 3, pp. 323–325, 2010.

[39] A. M. Chrysler, C. M. Furse, K. L. Hall, and Y. Chung, "Effect of material properties on a subdermal UHF RFID antenna," *IEEE J. Radio Freq. Identif.*, vol. 1, no. 4, pp. 260–266, Dec. 2017.

[40] N. Roy, A. Trivedi, and J. Wong, "Designing an FPGA-Based RFID Reader," *XCell J.*, vol. 2, pp. 26–29, 2nd Quart., 2006.

[41] K. H. Lee *et al.*, "Design of a UHF RFID metal tag for long reading range using a cavity structure," in *Proc. Asia–Pac. Microw. Conf.*, Macau, China, 2008, pp. 1–4

[42] G. Kramer, M. Gastpar, and P. Gupta, "Cooperative strategies and capacity theorems for relay networks," *IEEE Trans. Inf. Theory*, vol. 51, no. 9, pp. 3037–3063, Sep. 2005.

[43] R. U. Nabar, H. Bolcskei, and F. W. Kneubuhler, "Fading relay channels: Performance limits and space-time signal design," *IEEE J. Sel. Areas Commun.*, vol. 22, no. 6, pp. 1099–1109, Aug. 2004.

[44] M. Baghaei-Nejad, Z. Zou, H. Tenhunen, and L. R. Zheng, "A novel passive tag with asymmetric wireless link for RFID and WSN applications," in *Proc. IEEE Int. Symp. Circuits Syst.*, New Orleans, LA, USA, 2007, pp. 1593–1596.

[45] Y. Karimi, A. Athalye, S. R. Das, P. M. Djurić, and M. Stanaćević, "Design of a backscatter-based tag-to-tag system," in *Proc. IEEE Int. Conf. RFID (RFID)*, Phoenix, AZ, USA, 2017, pp. 6–12.

[46] Z. J. Haas and Z. Zheng, "Waveform design for RF power transfer," U.S. Patent 15 959 917, Nov. 2018.

[47] C. Deng, Y. Li, Z. Zhang, and Z. Feng, "A wideband isotropic radiated planar antenna using sequential rotated L-shaped monopoles," *IEEE Trans. Antennas Propag.*, vol. 62, no. 3, pp. 1461–1464, Mar. 2014.

[48] Y. Maguire and R. Pappu, "An optimal Q-algorithm for the ISO 18000-6C RFID protocol," *IEEE Trans. Autom. Sci. Eng.*, vol. 6, no. 1, pp. 16–24, Jan. 2009.

[49] G. Marrocco, "The art of UHF RFID antenna design: Impedance-matching and size-reduction techniques," *IEEE Antennas Propag. Mag.*, vol. 50, no. 1, pp. 66–79, Feb. 2008.

[50] C. Floerkemeier and S. Sarma, "RFIDSim—A physical and logical layer simulation engine for passive RFID," *IEEE Trans. Autom. Sci. Eng.*, vol. 6, no. 1, pp. 33–43, Jan. 2009.

[51] N. C. Karmaker, "Tag, you're it radar cross section of chipless RFID tags," *IEEE Microw. Mag.*, vol. 17, no. 7, pp. 64–74, Jul. 2016.

[52] G. Andíia Vera, Y. Duroc, and S. Tedjini, "Third harmonic exploitation in passive UHF RFID," *IEEE Trans. Microw. Theory Techn.*, vol. 63, no. 9, pp. 2991–3004, Sep. 2015.

[53] J. Lee and B. Lee, "A long-range UHF-band passive RFID tag IC based on high- Q design approach," *IEEE Trans. Ind. Electron.*, vol. 56, no. 7, pp. 2308–2316, Jul. 2009.

[54] R. Chakraborty, S. Roy, and V. Jandhyala, "Revisiting RFID link budgets for technology scaling: Range maximization of RFID tags," *IEEE Trans. Microw. Theory Techn.*, vol. 59, no. 2, pp. 496–503, Feb. 2011.

[55] P. V. Nikitin, K. V. S. Rao, R. Martinez, and S. F. Lam, "Sensitivity and Impedance Measurements of UHF RFID Chips," *IEEE Trans. Microw. Theory Techn.*, vol. 57, no. 5, pp. 1297–1302, May 2009.

[56] G. De Vita and G. Iannaccone, "Design criteria for the RF section of UHF and microwave passive RFID transponders," *IEEE Trans. Microw. Theory Techn.*, vol. 53, no. 9, pp. 2978–2990, Sep. 2005.

[57] A. P. Sample, D. J. Yeager, P. S. Powledge, A. V. Mamishev, and J. R. Smith, "Design of an RFID-based battery-free programmable sensing platform," *IEEE Trans. Instrum. Meas.*, vol. 57, no. 11, pp. 2608–2615, Nov. 2008.

[58] L. Catarinucci, D. De Donno, R. Colella, F. Ricciato, and L. Tarricone, "A cost-effective SDR platform for performance characterization of RFID tags," *IEEE Trans. Instrum. Meas.*, vol. 61, no. 4, pp. 903–911, Apr. 2012.

[59] T. Yang *et al.*, "An active tag using carrier recovery circuit for EPC Gen2 passive UHF RFID systems," *IEEE Trans. Ind. Electron.*, vol. 65, no. 11, pp. 8925–8935, Nov. 2018.

[60] S. Merilampi, T. Björninen, L. Ukkonen, P. Ruuskanen, and L. Sydänheimo, "Embedded wireless strain sensors based on printed RFID tag," *Sens. Rev.*, vol. 31, no. 1, pp. 32–40, 2011.

[61] A. P. Parra, J. J. Pantoja, E. Neira, and F. Vega, "On the backscattering from RFID tags installed on objects," in *Proc. 10th Eur. Conf. Antennas Propag. (EuCAP)*, Davos, Switzerland, Apr. 2016, pp. 1–5.

[62] P. V. Nikitin and K. V. S. Rao, "Theory and measurement of backscattering from RFID tags," *IEEE Antennas Propag. Mag.*, vol. 48, no. 6, pp. 212–218, Dec. 2006.

[63] P. V. Nikitin, K. V. S. Rao, and S. Lazar, "An overview of near field UHF RFID," in *Proc. IEEE Int. Conf. RFID*, Grapevine, TX, USA, 2007, pp. 167–174.

[64] T. P. Ketterl, R. A. Ramirez, and T. M. Weller, "Reduced-size circular polarized antenna for 434MHz RFID systems using meandered bowtie elements with a novel quadrifilar feed," in *Proc. IEEE 16th Annu. Wireless Microw. Technol. Conf. (WAMICON)*, Cocoa Beach, FL, USA, 2015, pp. 1–3.

[65] G. A. Casula, G. Montisci, and G. Mazzarella, "A wideband PET inkjet-printed antenna for UHF RFID," *IEEE Antennas Wireless Propag. Lett.*, vol. 12, pp. 1400–1403, 2013.

[66] A. Safarian, A. Shameli, A. Rofougaran, M. Rofougaran, and F. De Flaviis, "RF identification (RFID) reader front ends with active blocker rejection," *IEEE Trans. Microw. Theory Techn.*, vol. 57, no. 5, pp. 1320–1329, May 2009.

[67] P. V. Nikitin and K. V. S. Rao, "LabVIEW-based UHF RFID tag test and measurement system," *IEEE Trans. Ind. Electron.*, vol. 56, no. 7, pp. 2374–2381, Jul. 2009.

[68] A. E. Abdulhadi and R. Abhari, "Multiport UHF RFID-tag antenna for enhanced energy harvesting of self-powered wireless sensors," *IEEE Trans. Ind. Informat.*, vol. 12, no. 2, pp. 801–808, Apr. 2016.

[69] P. B. Khannur *et al.*, "A universal UHF RFID reader IC in 0.18-μm CMOS technology," *IEEE J. Solid-State Circuits*, vol. 43, no. 5, pp. 1146–1155, May 2008.

[70] H. Chung, H. Mo, N. Kim, and C. Pyo, "An advanced RFID system to avoid collision of RFID reader, using channel holder and dual sensitivities," *Microw. Opt. Technol. Lett.*, vol. 49, pp. 2643–2647, Nov. 2007.

[71] P. Pursula, F. Donzelli, and H. Seppa, "Passive RFID at millimeter waves," *IEEE Trans. Microw. Theory Techn.*, vol. 59, no. 8, pp. 2151–2157, Aug. 2011.

[72] C. Yao and W. Hsia, "A–21.2 -dBm dual-channel UHF passive CMOS RFID tag design," *IEEE Trans. Circuits Syst. I, Reg. Papers*, vol. 61, no. 4, pp. 1269–1279, Apr. 2014.

[73] A. Bekkali, S. Zou, A. Kadri, M. Crisp, and R. V. Penty, "Performance analysis of passive UHF RFID systems under cascaded fading channels and interference effects," *IEEE Trans. Wireless Commun.*, vol. 14, no. 3, pp. 1421–1433, Mar. 2015.

[74] J. Park, J. Jung, S. Ahn, H. Roh, H. Oh, Y. Seong, Y. Lee, and K. Choi, "Extending the interrogation range of a passive UHF RFID system with an external continuous wave transmitter," *IEEE Trans. Instrum. Meas.*, vol. 59, no. 8, pp. 2191–2197, Aug. 2010.

[75] C. Yao and W. Hsia, "An indoor positioning system based on the dual-channel passive RFID technology," *IEEE Sensors J.*, vol. 18, no. 11, pp. 4654–4663, Jun. 2018.

[76] J. Jung, C. Park, and K. Yeom, "A novel carrier leakage suppression front-end for UHF RFID reader," *IEEE Trans. Microw. Theory Techn.*, vol. 60, no. 5, pp. 1468–1477, May 2012.

[77] R. Z. Doany, C. Lovejoy, K. Jones, and H. Stern, "A CDMA-based RFID inventory system: A CDMA approach as a solution for decreased power consumption," in *Proc. IEEE Int. Conf. RFID (RFID)*, Orlando, FL, USA, 2016, pp. 175–178.